Dinuclear Nickel(II) Complexes as Models for the Active Site of Urease

Dirk Volkmer,[†] Birgit Hommerich,[†] Klaus Griesar,[‡] Wolfgang Haase,[‡] and Bernt Krebs*,[†]

Anorganisch-Chemisches Institut der Universität Münster, Wilhelm-Klemm-Strasse 8, D-48149 Münster, Germany, and Institut für Physikalische Chemie, Technische Hochschule Darmstadt, D-64287 Darmstadt, Germany

Received December 7, 1995[⊗]

Dinuclear nickel(II) complexes of the ligands 2,6-bis[bis((2-benzimidazolylmethyl)amino)methyl]-*p*-cresol (bbapOH), *N*,*N*,*N*′,*N*′-tetrakis(2-benzimidazolylmethyl)-2-hydroxy-1,3-diaminopropane (tbpOH), *N*-methyl-*N*,*N*′,*N*′-tris(2-benzimidazolylmethyl)-2-hydroxy-1,3-diaminopropane (m-tbpOH) and 1-[*N*,*N*-bis(2-benzimidazolylmethyl)-amino]-3-[2-(3,5-dimethyl-1*H*-pyrazol-1-yl)ethoxy]-2-hydroxypropane (bpepOH) were prepared in order to model the active site of urease. The novel asymmetric structures of the dinuclear complexes were characterized by X-ray structure analysis. The complex $[Ni_2(bbapO)(ClO_4)(H_2O)(MeOH)](ClO_4)_2 \cdot Et_2O$, **1**, crystallizes in the monoclinic space group $P2_1/c$, with $a = 10.258(2)$ Å, $b = 19.876(3)$ Å, $c = 25.592(4)$ Å, and $\beta = 97.12(2)°$. The nickel ions in **1** are bridged by the phenoxy donor of the ligand and a perchlorate anion. The complexes $[Ni_2(tbpO)(MeCOO)(H_2O)](ClO_4)_2 \cdot H_2O \cdot Et_2O$, **2**, $[Ni_2(m\text{-}tbpO)(PhCOO)(EtOH)_2](ClO_4)_2 \cdot EtOH$, **3**, and $[Ni_2(bpepO)(MeCOO)(H_2O)_2](ClO_4)_2 \cdot H_2O \cdot Et_2O \cdot 2EtOH$, **4**, also crystallize in the monoclinic crystal system with the following unit cell parameters: **2**, *C*2/*c*, $a = 35.360(13)$ Å, $b = 10.958(3)$ Å, $c = 24.821(10)$ Å, $\beta = 103.55(3)°$; **3**, *Cc*, $a = 14.663(5)$ Å, $b = 32.630(13)$ Å, $c = 9.839(3)$ Å, $\beta = 92.49(2)°$; **4**, *C*2/*c*, $a = 27.689(13)$ Å, $b = 12.187(5)$ Å, $c = 31.513(14)$ Å, $\beta = 115.01(3)°$. The dinuclear centers of all these complexes are bridged by the alkoxy donor of the ligand and a carboxylate function. Compounds **2** and **3** have one of the nickel ions in a five-coordinated, trigonal bipyramidal coordination environment and thus show a high structural similarity to the dinuclear active site of urease from *Klebsiella aerogenes*. Furthermore, their magnetic and spectroscopic properties were determined and related to those of the urease enzymes. Activity toward hydrolysis of test substrates (4-nitrophenyl)urea, 4-nitroacetanilide, 4-nitrophenyl phosphate or bis(4-nitrophenyl) phosphate by the dinuclear complexes were examined by UV spectroscopic measurements.

Introduction

The quest for the structure and the principal function of the dinuclear active site of the nickel containing enzyme urease (urea amidohydrolase, EC 3.5.1.5) has attracted the attention of both biochemists and inorganic chemists for 70 years.[1] Although urease from jack beans was isolated in the crystalline state in early 1926 by Sumner,[2] it was only shown in 1975 that the enzyme contains stoichiometric amounts of Ni(II) ions.[3] Nickel-dependent ureases may also be obtained from microorganisms,[4] and the comparison of the amino acid sequences of a variety of microbial ureases with that of the plant enzyme has shown surprising sequence homology with a highly conserved region of 20 amino acid residues within the primary structures.[5]

The widely accepted mechanism for urea hydrolysis was suggested by Zerner *et al.* in which two Ni(II) ions are involved in the catalytic cycle.[6] In the key step of the proposed mechanism, a coordinated hydroxide ion attacks the carbonyl C atom of the urea substrate which is coordinated to the opposite Ni(II) ion to form a bridging tetrahedral intermediate. The binding sites for the metal ions have to be different to attain directed specifity in the catalytic cycle. The recently determined structure of the microbial urease from *Klebsiella aerogenes* provides clear evidence for a dinickel active site in which the two nickel ions are 3.5 Å apart.[7] The metal ions are bridged by the carboxylate function of a carbamylated lysine residue. The coordination of Ni(1) is pseudotetrahedral with two histidine nitrogens, the oxygen of the bridging carbamate and a water molecule. The coordination geometry for Ni(2) is described as trigonal bipyramidal with a further asparagine oxygen completing the first coordination shell. The low coordination numbers of both nickel ions contrast in some ways the predictions of earlier spectroscopic and magnetochemical studies where the metal ions have been described to be five- or six-coordinated within a mixed nitrogen−oxygen donor environment.[8]

On the basis of these studies, we have tried to model the properties of the dinuclear active site of ureases. The general strategy was to synthesize dinickel complexes of both symmetric

* To whom correspondence should be addressed.
[†] Universität Münster.
[‡] Technische Hochschule Darmstadt.
[⊗] Abstract published in *Advance ACS Abstracts,* May 15, 1996.

(1) For comprehensive reviews see: (a) Blakeley, R. L.; Zerner, B *J. Mol. Catal.* **1984**, *23*, 263. (b) Andrews, R. K.; Blakeley, R. L.; Zerner, B. *Met. Ions Biol. Syst.* **1988**, *23*, 186. (c) Mobley, H. L. T.; Hausinger, R. P. *Microbiol. Rev.* **1989**, *53*, 85. (d) Kolodziej, A. F. *Prog. Inorg. Chem.* **1994**, *41*, 493.
(2) Sumner, J. B. *J. Biol. Chem.* **1926**, *69*, 435.
(3) (a) Dixon, N. E.; Gazzola, C.; Watters, J. J.; Blakeley, R. L.; Zerner, B. *J. Am. Chem. Soc.* **1975**, *97*, 4130. (b) Dixon, N. E.; Gazzola, C.; Blakeley, R. L.; Zerner, B. *J. Am. Chem. Soc.* **1975**, *97*, 4131.
(4) (a) Todd, M. J.; Hausinger, R. P. *J. Biol. Chem.* **1987**, *262*, 5963. (b) Breitenbach, J. M.; Hausinger, R. P. *Biochem. J.* **1988**, *250*, 917. (c) Jones, B. D.; Mobley, H. L. T. *J. Bacteriol.* **1988**, *170*, 3342. (d) Hu, L.-T.; Mobley, H. L. T. *Infect. Immun.* **1990**, *58*, 992.
(5) Sriwanthana, B.; Mobley, H. L. T. *Infect. Immun.* **1993**, *61*, 2570.
(6) Dixon, N. E.; Riddles, P. W.; Gazzola, C.; Blakeley, R. L.; Zerner, B. *Can. J. Biochem.* **1980**, *58*, 1335; *Erratum. Ibid.* **1981**, *59*, 564.
(7) Jabri, E.; Carr, M. B.; Hausinger, R. P.; Karplus, P. A. *Science* **1995**, *268*, 998.
(8) (a) Wang, S.; Lee, M. H.; Hausinger, R. P.; Clark, P. A.; Wilcox, D. E.; Scott, R. A. *Inorg. Chem.* **1994**, *33*, 1589. (b) Day, E. P.; Peterson, J.; Sendova, M. S.; Todd, M. J.; Hausinger, R. P. *Inorg. Chem.* **1993**, *32*, 634. (c) Clark, P. A.; Wilcox, D. E. *Inorg. Chem.* **1989**, *28*, 1326. (d) Clark, P. A.; Wilcox, D. E.; Scott, R. A. *Inorg. Chem.* **1990**, *29*, 579. (e) Blakeley, R. L.; Dixon, N. E.; Zerner, B. *Biochim. Biophys. Acta* **1983**, *744*, 219. (f) Alagna, L.; Hasnain, S. S.; Piggott, B.; Williams, D. J. *Biochem. J.* **1984**, *220*, 591.

S0020-1669(95)01567-9 CCC: $12.00

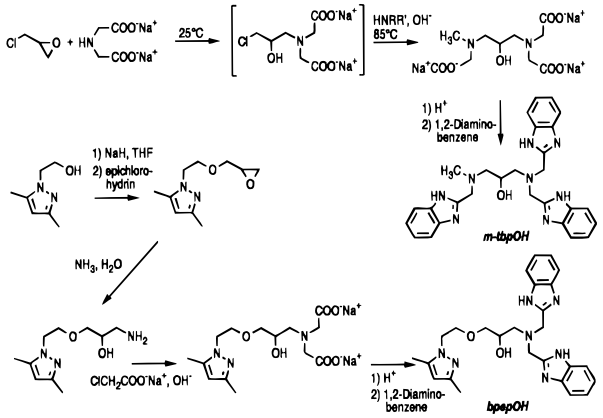

Figure 1. Reaction scheme for the synthesis of the asymmetric, dinucleating ligands m-tbpOH and bpepOH.

and asymmetric polydentate ligands which may predefine an appropriate orientation of the substrate and the attacking nucleophile and thus limit the possible reactions that occur at the "free" coordination sites. We recently reported the synthesis of an asymmetric dinuclear Ni(II) complex which we have described as a structure model for the active site of urease in its substrate-bound form.[9] In the light of developing hydrolytically active compounds, we now describe the synthesis, X-ray structures, and spectroscopic and magnetic properties of four structurally different dinickel complexes which all have readily displaceable, monodentate ligands. As a test for their different reactivities, titrations using 2-hydroxyethanethiolate as a spectroscopic probe were performed. Furthermore, the compounds were tested for their ability to hydrolyze a variety of substrates. Compound $[Ni_2(bpepO)(MeCOO)(H_2O)_2](ClO_4)_2 \cdot H_2O \cdot Et_2O \cdot 2EtOH$, **4**, shows an accelerated hydrolysis of the substrate 4-nitrophenyl phosphate. The relevance of the complexes to mimic different states of the active site of urease is finally discussed.

Experimental Section

Preparations. Unless otherwise stated all starting materials were purchased from commercial sources and were used without further purification. Solvents were dried using standard laboratory techniques. Melting points were determined by using a Mettler melting point apparatus (FP 51) and are uncorrected. Elemental analyses were performed on a Hewlett-Packard Scientific Model 185. ^{1}H and ^{13}C NMR spectra were recorded on Bruker WH300 and WH90 spectrometers. ^{1}H chemical shifts of the compounds are related to TMS as an internal standard of the deuterated solvent. IR spectra of the metal complexes were measured as KBr pressings on a Perkin Elmer 683 spectrometer. The symmetric ligands 2,6-bis[(bis(2-benzimidazolylmethyl)amino)methyl]-*p*-cresol (bbapOH) and *N*,*N*,*N*′,*N*′-tetrakis(2-benzimidazolylmethyl)-2-hydroxy-1,3-diaminopropane (tbpOH) were synthesized according to published procedures.[10,11] Asymmetric ligands were prepared by following the synthetic routes presented in Figure 1.

***N*-Methyl-*N*,*N*′,*N*′-tris(2-benzimidazolylmethyl)-2-hydroxy-1,3-diaminopropane (m-tbpOH). (a) *N*-[3-[Bis(carboxymethyl)amino]-2-hydroxypropyl]-*N*-methylglycine.** A cooled solution of NaOH (2.4 g, 0.06 mol) in 10 mL of water was added to a stirred suspension of iminodiacetic acid (4.0 g, 0.03 mol) in 10 mL of water. To this cooled solution was added epichlorohydrine (2.4 mL, 0.03 mol). The dispersion was stirred at room temperature until a clear solution resulted (ca. 90 min). Then, a solution of *N*-methylglycine (2.7 g, 0.03 mol) and NaOH (1.2 g, 0.03 mol) in 10 mL of water was added at once, and the reaction mixture was heated to 85 °C. When the final temperature was reached a solution of NaOH (1.2 g, 0.03 mol) in 10 mL of water was added dropwise over a time period of about 1 h. The reaction mixture was stirred for another hour at 85 °C. Finally, a 70% aqueous solution of perchloric acid (12.9 g, 0.09 mol) in 10 mL of water was added, and the reaction mixture was slowly cooled down to room temperature. Precipitation of the triacid was completed by leaving the suspension for 3 days at 0 °C. The very fine white precipitate was filtered off and recrystallized three times from 60 mL portions of water. The product was dried at 60 °C to yield 5.4 g of *N*-[3-[bis-(carboxymethyl)amino]-2-hydroxypropyl]-*N*-methylglycine. (65%). Mp: 221 °C. Anal. Calcd for $C_{10}H_{18}N_2O_7$: C, 43.16; H, 6.52; N, 10.07. Found: C, 43.47; H, 6.30; N, 10.01. ^{1}H NMR (D_2O, KOH, 363 K): δ 4.43−4.38 (m, 1H), 3.79 (s, 4H), 3.61 (s, 2H), 3.32−3.27 (m, 1H), 3.07−3.01 (m, 3H), 2.86 (s, 3H) ppm. (*Note*: Addition of the amino acid components in reversed succession resulted in significantly lower yields.)

(b) m-tbpOH. *N*-[3-[Bis(carboxymethyl)amino]-2-hydroxypropyl]-*N*-methylglycine (3.48 g, 0.0125 mol) and 1,2-diaminobenzene (4.05 g, 0.0375 mol) were finely ground, mixed together, and heated up to 180 °C, until the evolution of gas had ceased (ca. 2 h). The dark residue was dissolved in refluxing ethanol (100 mL) and treated repeatedly with active charcoal until the filtrate was nearly colorless. The filtrate then was concentrated to half of the original volume and added dropwise to a solution of 10 mL of concentrated ammonia in 250 mL of hot water. The precipitated ligand was filtered off, and the residue was dried in vacuum for 2 h at 80 °C. The crude product was purified by flash chromatography on a silica column (eluent THF/MeOH 3:1; R_f 0.25) to yield 4.45 g of *N*-methyl-*N*,*N*′,*N*′-tris(2-benzimidazolylmethyl)-2-hydroxy-1,3-diaminopropane as a slightly yellow powder (72%). Mp: 123−125 °C. Anal. Calcd for $C_{28}H_{30}N_8O$: C, 68.00; H, 6.11; N, 22.66. Found: C, 68.20; H, 6.17; N, 22.42. ^{1}H NMR (DMSO-d_6): δ 7.53 (m, 6H), 7.14 (m, 6H), 4.16 (s, 4H), 3.96 (m, 1H), 3.83 (s, 2H), 2.88 (m, 1H), 2.73 (m, 1H), 2.55 (m, 2H), 2.26 (s, 3H) ppm. ^{13}C NMR (DMSO-d_6, 363 K): δ (isopropyl: 66.5 HO−*C*−H, 61.2 *C*H_2−N−(CH_3, CH_2−C_{ar}), 58.7 *C*H_2−N−(CH_2−C_{ar})$_2$); 42.4 N−*C*H_3, (2-benzimidazolylmethyl (A): 120.9, 114.3 C_{ar}−H, 152.5, 138.3 C_{ar}−q, 52.3 *C*H_2−C_{ar}); (2-benzimidazolylmethyl (B): 120.8, 114.3 C_{ar}−H, 152.2, 138.3 C_{ar}−q, 55.0 *C*H_2−C_{ar}) ppm.

1-[*N*,*N*-bis(2-benzimidazolylmethyl)amino]-3-[2-(3,5-dimethyl-1*H*-pyrazol-1-yl)ethoxy]-2-hydroxypropane (bpepOH). (a) 2-(3,5-Dimethyl-1*H*-pyrazol-1-yl)ethanol. 2-Hydrazinoethanol (5.1 g, 0.067 mol) was dissolved in 20 mL of methanol. The solution was cooled down to 0 °C. 1,3-Pentanedione (7.1 g, 0.071 mol) was added dropwise over a period of 90 min to the cooled solution. The solution was stirred overnight while slowly warming up to room temperature. The solvent was evaporated at 50 °C on a rotary evaporator, and the remaining viscous oil was taken up with 20 mL of ethyl acetate/20 mL of diethyl ether. The solution was kept at −22 °C for 24 h, and the white crystalline product was filtered off and washed with ether. The ether washings were combined with the filtrate to yield a second crop of 2-(3,5-dimethyl-1*H*-pyrazol-1-yl)ethanol after being cooled down to −22 °C. Total yield: 7.7 g (82%), Mp: 78 °C (lit.: 77 °C).[12] Anal. Calcd for $C_7H_{12}N_2O$: C, 59.97; H, 8.63; N, 19.98. Found: C, 59.78; H, 8.72; N, 19.87. ^{1}H NMR ($CDCl_3$): δ 5.79 (s, 1H), 4.02 (t, 2H), 3.93 (t, 2H), 2.22 (s, 3H), 2.19 (s, 3H) ppm.

(b) 3-[2-(3,5-Dimethyl-1H-pyrazol-1-yl)-1,2-epoxypropane. NaH (2.2 g, 0.05 mol, 55% in mineral oil) was washed three times with 15 mL of petroleum (Schlenk frit, Ar atmosphere). The resulting NaH was suspended in 35 mL of tetrahydrofuran. The suspension was cooled down to 0 °C, and 2-(3,5-dimethyl-1*H*-pyrazol-1-yl)ethanol (6.9 g, 0.049 mol) was added in small portions. Afterward, epichlorohydrine (8 mL, 0.1 mol) was added at once to the stirred solution. The temperature was raised to 60 °C within 1 h, and the reaction mixture was kept at this temperature for another 2 h. The solvent and excess of epichlorohydrine were distilled off under reduced pressure. The residue was taken up with 35 mL of diethyl ether and the suspension was cooled in an ice bath. 15 mL of water were added, and the aqueous phase was extracted three times with 10 mL portions of diethyl ether

(9) Volkmer, D.; Hörstmann, A.; Griesar, K.; Haase, W.; Krebs, B. *Inorg. Chem.* **1996**, *35*, 1132.
(10) Suzuki, M.; Kanatomi, H.; Murase, I. *Bull. Chem. Soc. Jpn.* **1984**, *57*, 36.
(11) McKee, V.; Zvagulis, M.; Dagdigian, J. V.; Patch, M. G.; Reed, C. A. *J. Am. Chem. Soc.* **1984**, *106*, 4765.
(12) Grandberg, I. I.; Sharova, G. I. *Khim. Geterosikl. Soedin* **1968**, *2*, 325; *Chem. Abstr.* **1968**, *69*, 96564k.

after the phases had separated. The combined organic extracts were dried over $MgSO_4$. The diethyl ether was stripped off at reduced pressure and the resulting yellow oil was distilled in vacuum to yield 6.5 g of 3-[2-(3,5-dimethyl-1*H*-pyrazol-1-yl)-1,2-epoxypropane (67.3%). Bp: 103−110 °C (0.5 mm). The product is a colorless oil which crystallizes when stored at −22 °C. At room temperature the product decomposes within a few days. Anal. Calcd for $C_{10}H_{16}N_2O_2$: C, 61.20; H, 8.22; N, 14.27. Found: C, 60.85; H, 8.09; N, 13.82. ^{1}H NMR ($CDCl_3$): δ 5.75 (s, 1H), 4.12 (t, 2H), 3.82 (m, 2H), 3.65 (dd, 1H), 3.30 (dd, 1H), 3.05 (m, 1H), 2.73 (dd, 1H), 2.52 (dd, 1H), 2.24 (s, 3H), 2.20 (s, 3H), ppm. ^{13}C NMR ($CDCl_3$): δ (3,5-dimethylpyrazolyl: 147.0, 139.4 C_{ar}−q, 104.4 C_{ar}−H, 12.0, 10.5 CH_3); (oxiranyl: 50.1 *C*H−O, 43.6 CH_2−O), 71.3, 70.0 CH_2−O, 48.0 CH_2−N_{ar}) ppm.

(c) 1-Amino-3-[2-(3,5-dimethyl-1*H*-pyrazol-1-yl)ethoxy]-2-hydroxypropane. 3-[2-(3,5-Dimethyl-1*H*-pyrazol-1-yl)ethoxy]-1,2-epoxypropane (5.83 g, 0.03 mol) was added to 50 mL of concentrated ammonia solution. The reaction mixture was stirred for 12 h until the solution became clear. Finally the solution was heated at 80 °C for another 2 h. The excess of ammonia was removed on a rotary evaporator, and the highly viscous residue was distilled in vacuum (bp: 150 °C, 0.1 mm) to yield 4.62 g of 1-amino-3-[2-(3,5-dimethyl-1*H*-pyrazol-1-yl)ethoxy]-2-hydroxypropane (73.3%) as a colorless oil that slowly solidified on standing at room temperature. The product is very hygroscopic. Mp: 53−55 °C. Anal. Calcd for $C_{10}H_{19}N_3O_2$: C, 56.32; H, 8.98; N, 19.70. Found: C, 55.89; H, 9.03; N, 20.45. ^{1}H NMR ($CDCl_3$): δ 5.69 (s, 1H), 4.03 (t, 2H), 3.72 (t, 2H), 3.59−3.54 (m, 1H), 3.36−3.30 (m, 2H), 2.66−2.52 (m, 2H), 2.14 (s, 3H), 2.11 (s, 3H) ppm.

(d) bpepOH. 2-Chloroacetic acid (0.95 g, 0.01 mol) was dissolved in 2 mL of water. On cooling in an ice bath, a solution of NaOH (0.4 g, 0.01 mol) in 3 mL of water was added slowly such that the temperature of the reaction mixture was kept below 20 °C.

1-Amino-3-[2-(3,5-dimethyl-1*H*-pyrazol-1-yl)-ethoxy]-2-hydroxypropane (1.07 g, 5 mmol) was added and the solution was heated up to 65 °C. When the mixture reached the final temperature, a solution of NaOH (0.4 g, 0.01 mol) in 3 mL of water was added slowly (approximately 1 h). The mixture was stirred for another 3 h at 65 °C. Then an excess of 6 M hydrochloric acid (5 mL) was added at once. The solvent was evaporated under reduced pressure. The residue was refluxed in ethanol and the sodium chloride was filtered off. The filtrate was evaporated to dryness and the procedure was repeated until no further sodium chloride precipitation occured. Finally the solution was evaporated to dryness to yield *N*-[1-[bis(carboxymethyl)amino]-3-[2-(3,5-dimethyl-1*H*-pyrazol-1-yl)ethoxy]-2-hydroxypropane hydrochloride ($C_{14}H_{23}N_3O_6$·HCl). The product was mixed with 2 equiv of 1,2-diaminobenzene and the mixture was heated up to 180 °C for 2 h. The residue was dissolved in 10 mL of ethanol, and the solution was treated with active charcoal until the filtrate was nearly colorless. Further workup was essentially the same as in the case of the ligand m-tbpOH. BpepOH was obtained as a slightly yellow powder in more than 95% purity. Yield: 1.00 g (84.9%). Anal. Calcd for $C_{26}H_{31}N_7O_2$: C, 65.94; H, 6.60; N, 20.70. Found: C, 64.30; H, 6.91; N, 19.83. ^{1}H NMR (DMSO-d_6): δ 7.57−7.54 (m, 4H), 7.18−7.15 (m, 4H), 5.61 (s, 1H), 4.06 (s, 4H), 3.88 (t, 2H), 3.78 (m, 1H), 3.58 (t, 2H), 3.28 (m, 2H), 2.68 (m, 2H), 2.01 (s, 3H), 1.99 (s, 3H) ppm. ^{13}C NMR (DMSO-d_6): δ (3,5-dimethylpyrazolyl: 145.9, 138.7 C_{ar}−q, 104.5 C_{ar}−H, 13.4, 10.6 CH_3); (2-benzimidazolylmethyl: 121.6, 114.9 C_{ar}-H, 152.9, 139.3 C_{ar}−q, 52.7 CH_2−C_{ar}); 73.4, 66.8 CH_2−O, 69.9 HO−*C*−H, 57.4 CH_2−N, 47.9 CH_2−N_{ar} ppm.

[Ni_2(bbapO)(ClO_4)(H_2O)(MeOH)](ClO_4)$_2$·Et_2O (1). A sample of the ligand bbapOH (0.30 g, 0.42 mmol $C_{41}H_{38}N_{10}O$·HCl) was added in small portions to a solution of $[Ni(H_2O)_6](ClO_4)_2$ (0.329 g, 0.9 mmol) in 5 mL of 2-propanol. The solution was refluxed for about an hour when a green powder started to precipitate. The cooled solution was filtered and the microcrystalline solid was washed several times with diethyl ether. The product finally was dissolved in 3 mL of methanol. Slow vapor diffusion of diethyl ether into the solution gave dark green, platelike crystals of **1**. Yield: 0.250 g (49.2%). Anal. Calcd for $C_{46}H_{53}N_{10}Cl_3Ni_2O_{16}$: C, 45.07; H, 4.36; N, 11.43. Found: C, 43.60; H, 4.46; N, 11.00. IR (KBr, cm^{-1}): 3600−2800 (b, s), 1620 (b, w), 1600 (sh), 1540 (b, w), 1475 (s), 1450 (s), 1430 (m), 1390 (w), 1330 (w), 1305 (w), 1280 (m), 1230 (w), 1150−1070 (b, s), 1045 (m), 1005 (w), 955 (w), 945 (w), 920 (w), 875 (b, w), 850 (w), 790 (w), 765 (m), 750 (s), 635 (s), 625 (s).

[Ni_2(tbpO)(MeCOO)(H_2O)](ClO_4)$_2$·H_2O·Et_2O (2). $[Ni(H_2O)_6](ClO_4)_2$ (0.183 g, 0.5 mmol) and $[Ni(MeCOO)_2(H_2O)_4]$ (0.125 g, 0.5 mmol) were dissolved in 5 mL of hot methanol. To the hot solution was added tbpOH (0.305 g, 0.5 mmol $C_{35}H_{34}N_{10}O$) in small portions. The resulting dark green solution was added dropwise to a hot solution of $NaClO_4$·H_2O (1.0 g) in 10 mL of water. The suspension was cooled down to 0 °C while stirring. The dark green precipitate was isolated by filtration and washed several times with water. The crude product then was dissolved in 3 mL of methanol, and the solution was filtered through a sintered glass frit (D4 porosity). Diethyl ether was slowly diffused into the filtrate. After several days black green block-shaped crystals had formed. The crystallization was interrupted after 2 weeks, the crystals were filtered off, washed with ether, and air dried, yielding 0.134 g of **2** (24.4%). Anal. Calcd for $C_{41}H_{50}N_{10}Cl_2Ni_2O_{14}$: C, 44.96; H, 4.60; N, 12.79. Found: C, 43.49; H, 4.30; N, 12.73. IR (KBr, cm^{-1}): 3600−2800 (b, s), 1630 (sh), 1575 (s), 1545 (sh), 1500 (m), 1475 (s), 1455 (s), 1430 (sh), 1390 (sh), 1335 (m), 1285 (m), 1220 (w), 1160−1060 (b, s), 1045 (sh), 1005 (m), 980 (w), 950 (m), 925 (m), 905 (m), 850 (w), 765 (sh), 750 (s), 700 (b, m), 665 (m), 630 (s).

[Ni_2(m-tbpO)(PhCOO)(EtOH)$_2$](ClO_4)$_2$·EtOH (3). An ethanolic solution of m-tbpOH (0.247 g, 0.5 mmol $C_{28}H_{30}N_8O$) was added dropwise to a hot solution of $[Ni(H_2O)_6](ClO_4)_2$ (0.366 g, 1.0 mmol) and sodium benzoate (0.144 g, 1.0 mmol) in 5 mL of ethanol. The solution was refluxed for about 30 min. The cooled solution was filtered through a sintered glass frit. Slow vapor diffusion of diethyl ether into the filtrate gave dark green crystals of **3**. Yield: 0.210 g (39.3%). Anal. Calcd for $C_{41}H_{52}N_8Cl_2Ni_2O_{14}$: C, 46.06; H, 4.90; N, 10.48. Found: C, 45.64; H, 4.24; N, 10.69. IR (KBr, cm^{-1}): 3410 (b), 3063 (w), 2924 (m), 2855 (w), 1623 (w), 1565 (m), 1453 (s), 1400 (s), 1275 (m), 1117 (s), 1041 (s), 744 (s), 628 (m).

[Ni_2(bpepO)(MeCOO)(H_2O)$_2$](ClO_4)$_2$·H_2O·Et_2O·2EtOH (4). $[Ni(H_2O)_6](ClO_4)_2$ (0.183 g, 0.5 mmol) and $[Ni(MeCOO)_2(H_2O)_4]$ (0.125 g, 0.5 mmol) were dissolved in 5 mL of hot ethanol. To the hot solution bpepOH (0.237 g, 0.5 mmol $C_{26}H_{31}N_7O_2$) was added in small portions. The solution was filtered through a sintered glass frit (D4 porosity). Diethyl ether was slowly diffused into the filtrate. After several days green block-shaped crystals had formed. The crystallization was interrupted after 2 weeks, the crystals were filtered off, washed with ether, and air dried, yielding 0.286 g of **4** (53.4%). Anal. Calcd for $C_{36}H_{61}N_7Cl_2Ni_2O_{18}$: C, 40.48; H, 5.76; N: 9.18. Found: C, 38.04; H, 4.99; N, 9.72. IR (KBr, cm^{-1}): 3600−2800 (b, s), 1630 (sh), 1585 (s), 1560 (sh), 1500 (w), 1470 (sh), 1455 (s), 1435 (sh), 1395 (sh), 1335 (w), 1310 (w), 1285 (m), 1240 (w), 1160−1060 (b, s), 1050 (m), 1005 (w), 990 (w), 960 (w), 930 (w), 900 (w), 860 (w), 770 (sh), 750 (m), 675 (w), 640 (sh), 630 (s).

Caution! Perchlorate salts are potentially explosive and should only be handled in small quantities.

X-ray Crystallography. Crystal data as well as details of data collection and refinement are summarized in Table 1. Single crystals of compounds **1**−**4** were mounted on a glass fiber and placed on a Syntex $P2_1$ diffractometer (Mo Kα, λ = 0.710 73 Å, graphite monochromator). The crystals were immediately cooled by a stream of dry nitrogen gas to avoid aging by the loss of solvent molecules. Cell constants and orientation matrices were determined using least-squares refinements of the angular coordinates of at least 20 accurately centered reflections. Intensity data were collected by using the ω scan (**1**, **3**, and **4**) and the Wyckoff scan (**2**) techniques. As a check of crystal stability, two representative reflections were measured every 100 data points. No significant trend in their intensities was observed during the course of data acquisition. The intensity data were corrected for Lorentz and polarization factors, and an empirical absorption correction (**1**, **2**, and **4**) based on reflection measurements at different azimuthal angles was applied to the raw data. The structures were solved by using Patterson and Fourier methods (SHELXTL PLUS program package). Atomic scattering factors were taken from ref 13. The positions and anisotropic thermal parameters of all non-H atoms were refined against F_o^2 using full-matrix least-squares techniques (SHELXL-

(13) *International Tables for X-Ray Crystallography*, Kynoch Press: Birmingham, U.K., 1974; Vol. 4.

Table 1. Crystallographic and Refinement Data for $[Ni_2(bbapO)(ClO_4)(H_2O)(MeOH)](ClO_4)_2 \cdot Et_2O$, **1**, $[Ni_2(tbpO)(MeCOO)(H_2O)](ClO_4)_2 \cdot H_2O \cdot Et_2O$, **2**, $[Ni_2(m\text{-}tbpO)(PhCOO)(EtOH)_2](ClO_4)_2 \cdot EtOH$, **3**, and $[Ni_2(bpepO)(MeCOO)(H_2O)_2](ClO_4)_2 \cdot H_2O \cdot Et_2O \cdot 2EtOH$, **4**

	1	**2**	**3**	**4**
formula	$C_{46}H_{53}N_{10}Cl_3Ni_2O_{16}$	$C_{41}H_{50}N_{10}Cl_2Ni_2O_{14}$	$C_{41}H_{52}N_8Cl_2Ni_2O_{14}$	$C_{36}H_{61}N_7Cl_2Ni_2O_{18}$
M_w	1225.75	1095.23	1069.23	1068.24
cryst dimens, mm	0.08 × 0.12 × 0.25	0.15 ×0.34 × 0.38	0.24 × 0.22 × 0.12	0.35 × 0.37 × 0.22
radiation (λ, Å)	Mo Kα, (0.71073)	Mo Kα, (0.71073)	Mo Kα, (0.71073)	Mo Kα, (0.71073)
temp, K	170(2)	150(2)	150(2)	150(2)
space group	$P2_1/c$	$C2/c$	Cc	$C2/c$
a, Å	10.258(2)	35.360(13)	14.663(5)	27.689(13)
b, Å	19.876(3)	10.958(3)	32.630(13)	12.187(5)
c, Å	25.592(4)	24.821(10)	9.839(3)	31.513(14)
β, deg	97.12(2)	103.55(3)	92.49(2)	115.01(3)
V, Å^3	5178(2)	9350(6)	4703(3)	9637(7)
Z	4	8	4	8
D_{calc}, g/cm^3	1.572	1.556	1.510	1.473
μ, cm^{-1}	9.6	9.9	9.9	9.7
transm factor	0.74−0.73	0.85−0.83	0.84−0.78	0.86−0.76
index ranges	$0 \le h \le 11$, $0 \le k \le 22$, $-29 \le l \le 29$	$0 \le h \le 45$, $0 \le k \le 13$, $-31 \le l \le 30$	$0 \le h \le 16$, $0 \le k \le 37$, $-11 \le l \le 11$	$0 \le h \le 35$, $0 \le k \le 15$, $-40 \le l \le 36$
scan type	ω scan	Wyckoff scan	ω scan	ω scan
θ range, deg	2.05−24.06	2.07−27.00	2.33−24.05	2.11−27.06
no. of reflcns measd	8659	10355	3883	10743
no. of reflcns used	8156	10193	3883	10438
no of variables used	698	620	605	616
R [$nI > 2\sigma(I)$]	$R_1{}^a = 0.0508$, $wR_2{}^b = 0.1093$	$R_1{}^a = 0.0780$, $wR_2{}^b = 0.1873$	$R_1{}^a = 0.0436$, $wR_2{}^b = 0.0825$	$R_1{}^a = 0.0528$, $wR_2{}^b = 0.1214$
R (all data)	$R_1{}^a = 0.1058$, $wR_2{}^b = 0.1231$ $n = 4565$, $a^c = 0.0588$	$R_1{}^a = 0.1357$, $wR_2{}^b = 0.2239$ $n = 6128$, $a^c = 0.1295$	$R_1{}^a = 0.0656$, $wR_2{}^b = 0.0909$ $n = 3178$, $a^c = 0.0413$	$R_1{}^a = 0.1254$, $wR_2{}^b = 0.1548$ $n = 5270$, $a^c = 0.0717$
GOF on F^2	0.877	0.994	1.053	0.859

[a] $R_1 = \sum||F_o| - |F_c||/\sum|F_o|$. [b] $wR_2 = [\sum w(F_o^2 - F_c^2)^2/\sum wF_o^4]^{1/2}$. [c] $w = 1/[\sigma^2(F_o^2) + aP^2]$; $P = [\max(F_o^2, 0) + 2F_c^2]/3$.

93 program). Hydrogen atoms were included in calculated positions with their bonding distances and thermal parameters depending on the pivot atom (H−C(sp^2) 0.95 Å, $U_H = 1.2U_{eq}$(C); H−C(sp^3, CH_2-group) 0.99 Å, $U_H = 1.2U_{eq}$(C); H−C(sp^3, CH_3-group) 0.98 Å, $U_H = 1.5U_{eq}$-(C); H−N(sp^2) 0.88 Å, $U_H = 1.2U_{eq}$(N); H−O(sp^3) 0.84 Å, $U_H = 1.5U_{eq}$(O). The U_H values of H atoms belonging to solvent molecules were fixed to $U_H = 0.080$ Å^2). Positions of H atoms from possibly disordered structure fragments (e.g. CH_3 groups of acetate or tolyl, OH groups of (coordinated) water or alkanol molecules) were retrieved by examining the electron density map around the pivot atom. For acidic H atoms, possible H bonding contacts were taken into account to define their final positions.

Magnetic Susceptibility Measurements. Magnetic susceptibility measurements of powdered samples of compounds **1**−**4** were performed on a Faraday-type magnetometer consisting of a CAHN D-200 microbalance, a Leyboldt Heraeus VNK 300 helium flux cryostat, and a Bruker BE 25 magnet connected with a Bruker B-Mn 200/60 power supply in the temperature range 4−300 K. Experimental susceptibility data were corrected for the underlying diamagnetism. Magnetic moments were obtained from $\mu_{eff} = \mu_B(\chi T)^{1/2}$.

UV−Vis Spectroscopic Measurements and Kinetic Investigations. Electronic spectra of the complexes in the appropriate solvent were recorded on a Shimadzu UV 3100 PC spectrophotometer. The solutions of methanol and ethanol contained 0.01 M concentrations of the complexes and did not contain any buffers. The reflection spectra of the compounds were obtained by measuring the total reflectance of a powdered sample of the metal complexes diluted in $BaSO_4$ powder relative to a $BaSO_4$ standard.

Titrations of the complexes with 2-ME were performed directly in the UV cells. To 2.5 mL of the solution of the complex (0.001 M in MeOH) 50 μL volumes of solutions of 2-ME (0.01 M in MeOH) were pipetted. The measured spectra were corrected for the increase of the volume afterwards. Due to solubility problems no electrolyte for the standardization of the ionic strength could be applied. 2-ME was used as its mono sodium salt and it was assumed that the back dissociation of the thiolate anions in MeOH is negligible (pK_a(MeOH) = 16; pK_a-(2-ME) = 9.6).[14]

For hydrolysis tests, compounds **1**−**4** were dissolved in MeOH. Then 1 equiv of tetramethylammonium hydroxide (titer solution in MeOH) was slowly added to the metal complex solution with good stirring. The solutions were diluted with MeOH to a final concentration of 2×10^{-3} M. Then 2.5 mL of these solutions were pipetted into the thermostated UV cells and were left there for 2 h to equilibrate (60 °C, not corrected). Afterward, a volume of 50 μL of a methanolic solution of the test substrate was injected into the UV cell (concentration of the stock solution 5×10^{-3} M; concentration of the test substrate in the UV cell: 1×10^{-4} M; no corrections were applied for the increase in volume by heating or by the addition of the test substrate). The use of a 20-fold excess of the complex catalyst follows from two reasons. On the one hand the reaction should proceed with a rate law that obeys a pseudo-first-order kinetics to simplify the analysis of the measurements. On the other hand the excess of (coordinated) hydroxide anions compensates for the missing pH buffering that would be neccessary to shift the pH-dependent equilibrium of the hydrolysis products (4-nitrophenol and 4-nitrophenolate) to the side of the more easily detectable phenolate anion ($\lambda_{max} = 400$ nm, $\epsilon_{max} = 19\,200$ M^{-1} cm^{-1}).[15] For the estimation of hydrolysis activity, the increase of the absorption at wavelength of 400 nm (370 nm respectively) was monitored for a period of about 30 min. The test substrates behaved identically and did not show any detectable hydrolysis during 30 min when they were reacted with 20 equiv of tetramethylammonium hydroxide at 60 °C. Thus, corrections for their spontaneous hydrolysis were unnecessary. The rate constant k_o of the reaction of the active complex **4** with pnpp was determined from initial-rate experiments.[16]

The increase of the absorption at 400 nm was monitored for a time period of 30 min for different starting concentrations of the catalyst. The curves were fitted by a polynomial regression using four terms. The coefficient of the linear term then yielded the initial rate of the reactions for different concentrations of the catalysts. A plot of the observed rate constants k_o vs the starting concentration c_0 of the catalyst allowed us to determine the order in concentration of the catalyst. Since we could not find a significantly better fit assuming the reaction law

(14) (a) Todd, M. J.; Hausinger, R. P. *J. Biol. Chem.* **1989**, *264*, 15835. (b) Unmack, A. Z. *Phys. Chem.* **1928**, *133*, 45.

(15) Although the hydrolysis product 4-nitroaniline is not dissociated in the pH-range of 7−12 we applied a 20-fold excess of the catalyst with the substrates pnaa and pnpu to ensure a significant hydrolysis reaction within a reasonable time scale. λ_{max} (pna) = 370 nm, ϵ_{max} = 17 500 M^{-1} cm^{-1}.

(16) Wilkins, R. G. *Kinetics and Mechanism of Reactions of Transition Metal Complexes*; 2nd, thoroughly revised ed.; VCH:Weinheim, Germany, 1991; Chapters 1.2.1 and 3.

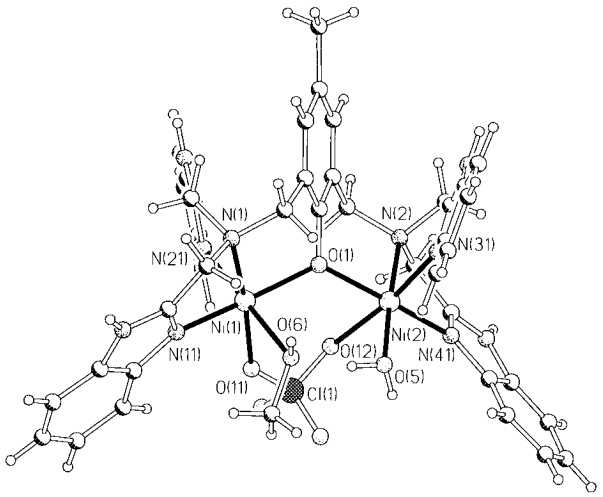

Figure 2. Structure of the cation of $[Ni_2(bbapO)(ClO_4)(H_2O)(MeOH)](ClO_4)_2 \cdot Et_2O$, **1**, with selected atomic designations.

to be of second- or third-order in the concentration of **4**, we used a linear approximation.[17]

Results and Discussion

Description of the X-ray Structures. $[Ni_2(bbapO)(ClO_4)(H_2O)(MeOH)](ClO_4)_2 \cdot Et_2O$ (1). Compound **1** crystallizes in the monoclinic space group $P2_1/c$. The structure of the cation of **1** is shown in Figure 2, and selected bond lengths and angles are given in Table 2. The Ni(II) ions in **1** are bridged by the phenoxy donor of the ligand bbapOH and a perchlorate anion. The Ni(1)···Ni(2) distance is 3.734(3) Å. Distortion of the local C_2 symmetry of the symmetric ligand results from the different coordination of the metal ions in which Ni(1) coordinates to a methanol molecule and Ni(2) to a water molecule respectively. The asymmetric coordination is due to a special hydrogen-bonding system in the crystal lattice. The water molecule forms strong, intramolecular hydrogen bonds to the methanolic oxygen (O(5)···O(6) = 2.655(4) Å) and to a terminal oxygen of the bridging perchlorate anion (O(5)···O(13) = 2.924(4) Å). The acidic proton of the coordinated methanol molecule respectively bonds to the oxygen of a noncoordinated perchlorate counteranion (O(6)···O(13) = 2.712(4) Å). The Ni(II)−O bond lengths of the coordinated water and the coordinated methanol molecule differ significantly (Ni(2)−O(5) = 2.037(4) Å; Ni(1)−O(6) = 2.236(4) Å). The difference may be rationalized in terms of an increase of the order of the Ni(II)−O bond of the water molecule which acts as a pure hydrogen donor. The methanol molecule also acts as a hydrogen donor but additionally takes part in the hydrogen bond to the opposite water molecule (net hydrogen acceptor).

Table 2. Selected Bond Lengths (Å) and Angles (deg) for **1**

Ni(1)··Ni(2)	3.734(3)	Ni(1)−O(11)	2.138(4)
		Ni(2)−N(2)	2.129(4)
Ni(1)−N(1)	2.122(4)	Ni(2)−N(31)	2.005(4)
Ni(1)−N(11)	2.046(4)	Ni(2)−N(41)	2.074(4)
Ni(1)−N(21)	2.024(4)	Ni(2)−O(1)	2.084(4)
Ni(1)−O(1)	2.051(3)	Ni(2)−O(5)	2.037(4)
Ni(1)−O(6)	2.236(4)	Ni(2)−O(12)	2.240(4)
Ni(1)−O(1)−Ni(2)	129.1(2)	N(2)−Ni(2)−N(41)	78.8(2)
		N(2)−Ni(2)−O(1)	93.0(2)
N(1)−Ni(1)−N(11)	79.3(2)	N(2)−Ni(2)−O(5)	176.4(2)
N(1)−Ni(1)−N(21)	84.4(2)	N(2)−Ni(2)−O(12)	90.4(2)
N(1)−Ni(1)−O(1)	91.1(2)	N(31)−Ni(2)−N(41)	98.4(2)
N(1)−Ni(1)−O(6)	94.2(2)	N(31)−Ni(2)−O(1)	90.0(2)
N(1)−Ni(1)−O(11)	173.8(1)	N(31)−Ni(2)−O(5)	96.2(2)
N(11)−Ni(1)−N(21)	95.9(2)	N(31)−Ni(2)−O(12)	172.0(2)
N(11)−Ni(1)−O(1)	168.1(2)	N(41)−Ni(2)−O(1)	167.4(2)
N(11)−Ni(1)−O(6)	83.6(2)	N(41)−Ni(2)−O(5)	97.8(2)
N(11)−Ni(1)−O(11)	94.5(2)	N(41)−Ni(2)−O(12)	85.4(2)
N(21)−Ni(1)−O(1)	90.1(2)	O(1)−Ni(2)−O(12)	85.2(1)
N(21)−Ni(1)−O(6)	178.6(2)	O(1)−Ni(2)−O(5)	90.6(2)
N(21)−Ni(1)−O(11)	97.1(2)	O(5)−Ni(2)−O(12)	90.3(2)
O(1)−Ni(1)−O(6)	90.1(1)		
O(1)−Ni(1)−O(11)	94.9(1)	O(11)−Cl(1)−O(12)	108.4(2)
O(6)−Ni(1)−O(11)	84.3(1)	Cl(1)−O(11)−Ni(1)	138.8(2)
N(2)−Ni(2)−N(31)	83.5(2)	Cl(1)−O(12)−Ni(2)	128.4(2)

The central six-membered ring consisting of the two Ni(II) ions, the phenolic oxygen and the chlorine and oxygen atoms of the bridging perchlorate anion has a folded chair conformation comparable to that of a distorted cyclohexane ring. The Cl−O bond lengths of the coordinated oxygen atoms of the bridging perchlorate anion are significantly longer (average Cl−O = 1.47 Å) than the terminal Cl−O bonds (average Cl−O = 1.42 Å). The coordination of the perchlorate anion may be described by a VB model in which the Cl−O bonds of the coordinated oxygen atoms have a decreased percentage of double bond character and an increased ionicity. In contrast, noncoordinated perchlorate anions show equal Cl−O bond lengths (average Cl−O = 1.42 Å) by means of equivalent weights of the VB resonance hybrids.

Dinuclear complexes of the ligand bbapOH have been described including the benzoate bridged dizinc and the dibenzylphosphate-bridged dicopper(II) moiety.[18a,b] Dinuclear complexes where exclusive bridging by the ligand occurs have been reported for Cu(II) and Cu(I) systems.[18c−e]

$[Ni_2(tbpO)(MeCOO)(H_2O)](ClO_4)_2 \cdot H_2O \cdot Et_2O$ (2). Complex **2** crystallizes in the monoclinic space group $C2/c$. The asymmetric unit contains a single formula unit. Further atoms are generated by the combination of a *c* glide plane parallel to (010) and a 2-fold axis parallel to *b*. Although the structure of the free ligand tbpOH is symmetric (point group C_s; O(1) and C(1) are situated in the mirror plane), the cation of **2** unexpectedly shows an asymmetric structure. Hence, the unit cell contains the racemic mixture of both enantiomers. The asymmetry is due to the different coordination of the two Ni(II) ions. The structure of the cation of **2** is shown in Figure 3, and selected bond lengths and angles are given in Table 3.

Ni(1) has trigonal bipyramidal coordination. The tertiary amine N(1) of the ligand and the oxygen O(51) of the bridging acetate occupy the axial positions. The trigonal basis is spanned by the atoms N(11), N(21), and O(1) of the ligand. The bond angles within the basis vary in the range 97.3(2)−131.4(2)°.

(17) The following equations were used to determine the rate constants of the hydrolysis experiments: (i) rate law obeying pseudo-first-order kinetics in the presence of a large excess of the catalyst: $v_o = d(c(\text{pnpat}))/dt = k_o c(\text{pnpat})$; (ii) polynomial approximation of the time course: $\text{abs}(t) = A_0 + A_1 t + A_2 t^2 + A_3 t^3$; (iii) Lambert−Beer law: $\text{abs}(\lambda,t) = l\sum_i \epsilon_i(\lambda) c_i(t)$. From (i), (ii), and (iii) follows: (iv) $v_0 = d(c(\text{pnpat}))/dt = A_1/\epsilon_{\text{pnpat}}$ with ϵ_{pnpat} being the molar extinction coefficient of pnpat at 400 nm under the experimental conditions. For determination abs(400 nm) was plotted against abs(307 nm). For abs(307 nm) = 0 the linear extrapolation of the data points yields the value for abs(400 nm) for "indefinitely" long reaction times: (v) $\epsilon_{\text{pnpat}} = \text{abs}(400)_{t\to\infty}/c_0(\text{pnpp})$. A plot of the observed rate constant k_o vs the starting concentration of the metal complex allows one to determine the order *m* of the catalyst in the rate law: (vi) $k_2 = k_o/c_o^m(\text{cat})$; Finally, the absorption curves were simulated using the determined values of ϵ_{pnpat} and k_2 within the integrated form of the pseudo-first-order rate law: (vii) $\text{abs}(t,400\text{ nm}) - \text{abs}(t_0, 400\text{ nm}) = c_0(\text{pnpp})\epsilon_{\text{pnpat}}(1 - \exp(-k_2 c_0^m(\text{cat}))$.

(18) (a) Uhlenbrock, S.; Krebs, B. *Angew. Chem.* **1992**, *104*, 1631; *Angew. Chem., Int. Ed. Engl.* **1992**, *31*, 1647. (b) Wall, M.; Hynes, R. C.; Chin, J. *Angew. Chem.* **1993**, *105*, 1696; *Angew. Chem., Int. Ed. Engl.* **1993**, *32*, 1633. (c) Berends, H. P.; Stephan, D. W. *Inorg. Chim. Acta* **1985**, *99*, L53. (d) Berends, H. P.; Stephan, D. W. *Inorg. Chem.* **1987**, *26*, 749. (e) Patch, M. G.; Hok-kin Choi; Chapman, D. R.; Bau, R.; McKee, V.; Reed, C. A. *Inorg. Chem.* **1990**, *29*, 110.

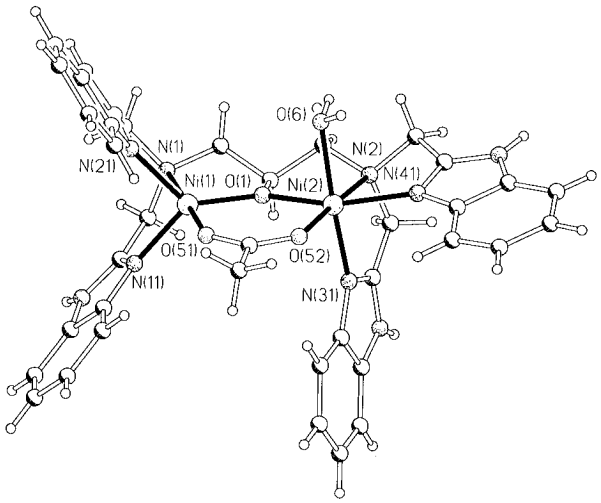

Figure 3. Structure of the cation of $[Ni_2(tbpO)(MeCOO)(H_2O)](ClO_4)_2 \cdot H_2O \cdot Et_2O$, **2**, with selected atomic designations.

Table 3. Selected Bond Lengths (Å) and Angles (deg) for **2**

Ni(1)···Ni(2)	3.521(4)	Ni(1)−O(51)	1.979(4)
Ni(1)···O(6)	3.904(4)	Ni(2)−N(2)	2.176(5)
		Ni(2)−N(31)	2.056(5)
Ni(1)−N(1)	2.184(5)	Ni(2)−N(41)	2.117(5)
Ni(1)−N(11)	2.008(5)	Ni(2)−O(1)	2.011(4)
Ni(1)−N(21)	1.998(5)	Ni(2)−O(6)	2.102(4)
Ni(1)−O(1)	1.902(4)	Ni(2)−O(52)	2.015(4)
Ni(1)−O(1)−Ni(2)	128.2(2)	N(1)−Ni(2)−O(52)	176.8(2)
		N(31)−Ni(2)−N(41)	93.1(2)
N(1)−Ni(1)−N(11)	80.2(2)	N(31)−Ni(2)−O(1)	92.4(2)
N(1)−Ni(1)−N(21)	82.0(2)	N(31)−Ni(2)−O(6)	172.7(2)
N(1)−Ni(1)−O(1)	83.6(2)	N(31)−Ni(2)−O(52)	94.8(2)
N(1)−Ni(1)−O(51)	179.7(2)	N(41)−Ni(2)−O(1)	159.1(2)
N(11)−Ni(1)−N(21)	97.3(2)	N(41)−Ni(2)−O(6)	86.0(2)
N(11)−Ni(1)−O(1)	125.4(2)	N(41)−Ni(2)−O(52)	102.1(2)
N(11)−Ni(1)−O(51)	99.6(2)	O(1)−Ni(2)−O(6)	86.0(2)
N(21)−Ni(1)−O(1)	131.4(2)	O(1)−Ni(2)−O(52)	97.5(2)
N(21)−Ni(1)−O(51)	97.8(2)	O(6)−Ni(2)−O(52)	92.4(2)
O(1)−Ni(1)−O(51)	96.7(2)		
N(1)−Ni(2)−N(31)	82.1(2)	O(51)−C(51)−O(52)	127.2(5)
N(1)−Ni(2)−N(41)	79.0(2)	C(51)−O(51)−Ni(1)	137.7(4)
N(1)−Ni(2)−O(1)	81.8(2)	C(51)−O(52)−Ni(2)	132.2(4)
N(1)−Ni(2)−O(6)	90.7(2)		

The coordination environment of Ni(2) is best described as that of a tetragonally distorted octahedron. Once again the tertiary amine group and the oxygen of the acetate (N(2), O(52)) take the axial positions. The basal plane is occupied by the atoms of the ligand and a neutral water molecule which is terminally coordinated. While the corresponding bond lengths of the nickel ions and the donor atoms in the axial positions are nearly identical in both subsets, the average distances of the basal coordinated atoms are shortened in the five-coordinated donor environment of Ni(1) (average Ni(1)−L = 2.01 Å; average Ni(2)−L = 2.08 Å). This may be rationalized in terms of reduced steric crowding that follows from a decrease in the number of coordinating atoms. The distance between the coordinated water molecule O(6) and the opposite Ni(1) is 3.904(4) Å. A further approach would lead to a symmetric bridging of the Ni(II) ions in the dinuclear unit. Also, coordination of a further water molecule to Ni(1) would result in a symmetric situation in which both of the metal ions are octahedrally coordinated. However, a change in the coordination environments would necessarily be accompanied by a change of the conformation of the central ring system containing the Ni(II) ions, the bridging alkoxo atom O(1) and the acetate anion. A linear correlation can be found between the folding angle φ of the ring system and the Ni···Ni distances. A detailed description of the changes in the structural parameters follows the description of the structures.

A similar asymmetric dimanganese(II) unit has recently been published in which the metal ions are bridged by an acetate anion and the octahedrally coordinated metal ion additionally coordinates an *n*-butanol molecule.[19a] However, ligand field stabilization for a high-spin d^8 metal ion should clearly prefer the octahedral vs the trigonal bipyramidal coordination environment, and the fact that the symmetric ligand tbpOH leads to both modes in the same dinuclear unit is not easily understood. A further asymmetric diiron(III) complex of the ligand tbpOH has been reported from our group.[19b] In this case, asymmetry is due to the coordination of different kinds of monodentate ligands, but both Fe(III) ions show an octahedral coordination geometry. Several dinuclear, *symmetric* complexes of tbpOH and benzimidazolyl-*N*-alkylated derivatives have been reported. In the case of Fe(II), trigonal bipyramidal coordination of both metal ions is observed.[19c,d] In contrast, diiron(III) complexes with acetate or benzoate bridging ligands exclusively show octahedral coordination of the metal ions.[19e,f] Related Cu(II) complexes with bridging acetate, azide, or nitrite contain the metal ions in either trigonal bipyramidal or square pyramidal coordination environments.[19g,h]

$[Ni_2(m\text{-}tbpO)(PhCOO)(EtOH)_2](ClO_4)_2 \cdot EtOH$ (3). Structure solution and refinement for compound **3** was performed in the space group *Cc*. The asymmetric unit contains a single formula unit; hence, both enantiomers of the asymmetric complexes are present in the unit cell. The coordination geometry of the Ni(II) ions in **3** is quite similar to the one that is found in **2**. This is surprising with respect to the diminished sterical constraints that could be expected for the coordination of the sterically less demanding ligand m-tbpOH. An overlay of the two cations of **2** and **3** that have the same absolute configuration at the asymmetric C(1) shows the coordination environments of the trigonal bipyramidal coordinated Ni(1) to be nearly identical. In **3** the positions that refer to the benzimidazolyl nitrogen donors N(31) and N(41) of compound **2** are now occupied by the oxygen donor atoms O(6) and O(7) of the coordinated solvent molecules. The corresponding nitrogen donor N(31) of the benzimidazolyl group of m-tbpOH then takes the position of the terminal water molecule O(6) in the cation of **2**. The central ring system consisting of the Ni(II) ions, the bridging alkoxo atom O(1) and the benzoate anion is similarly planar. The Ni···Ni distance of 3.514(3) Å is, within the estimated standard deviations, identical with the one that is observed for **2**. Similar to the terminal water molecule O(6) in **2**, the oxygen donor O(6) of the coordinated ethanol molecule is 3.972(3) Å away from the opposite Ni(1). A direct coordinative interaction between these two atoms thus can be ruled out. Asymmetric Cu(II) complexes of the ligand m-tbpOH have been recently described, but the ligand was prepared by a different, more complex synthetic route.[20] The structure of the cation of **3** is shown in Figure 4, and selected bond lengths and angles are given in Table 4.

(19) (a) Pessiki, P. J.; Khangulov, S. V.; Ho, D. M.; Dismukes, G. C. *J. Am. Chem. Soc.* **1994**, *116*, 891. (b) Bremer, B.; Schepers, K.; Fleischhauer, P.; Haase, W.; Henkel, G.; Krebs B. *J. Chem. Soc., Chem. Commun.* **1991**, *510*. (c) Ménage, S.; Brennan, B. A.; Juarez-Garcia, C.; Munck, E.; Que, L., Jr. *J. Am. Chem. Soc.* **1990**, *112*, 6423. (d) Yanhong Dong; Ménage, S.; Brennan, B. A.; Elgren, T. E.; Jang, Ho G.; Pearce, L. L.; Que, L., Jr. *J. Am. Chem. Soc.* **1993**, *115*, 1851. (e) Brennan, B. A.; Qiuhao Chen; Juarez-Garcia, C.; True, A. E.; O'Connor, C. J.; Que, L., Jr. *Inorg. Chem.* **1991**, *30*, 1937. (f) Qiuhao Chen; Lynch, J. B.; Gomez-Romero, P.; Ben-Hussein, A.; Jameson, G. B.; O'Connor, C. J.; Que, L., Jr. *Inorg. Chem.* **1988**, *27*, 2673. (g) McKee, V.; Dagdigian, J. V.; Bau, R.; Reed, C. A. *J. Am. Chem. Soc.* **1981**, *103*, 7000. (h) McKee, V.; Zvagulis, M.; Reed, C. A. *Inorg. Chem.* **1985**, *24*, 2914.

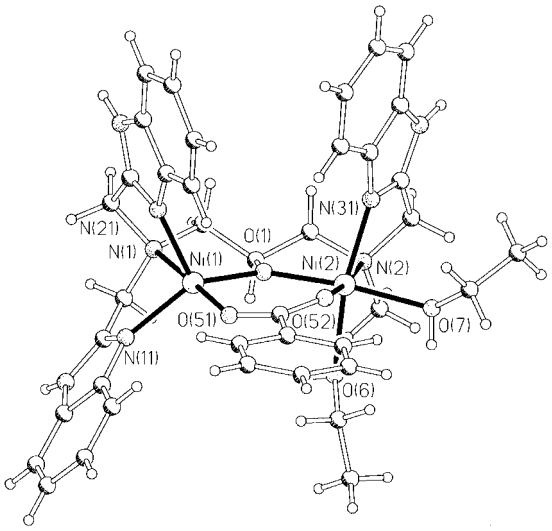

Figure 4. Structure of the cation of $[Ni_2(m\text{-}tbpO)(PhCOO)(EtOH)_2](ClO_4)_2 \cdot EtOH$, **3**, with selected atomic designations.

Table 4. Selected Bond Lengths (Å) and Angles (deg) for **3**

Ni(1)···Ni(2)	3.514(3)	Ni(1)−O(51)	2.021(5)
Ni(1)···O(6)	3.972(3)	Ni(2)−N(2)	2.164(6)
		Ni(2)−N(31)	2.071(7)
Ni(1)−N(1)	2.163(6)	Ni(2)−O(1)	1.974(5)
Ni(1)−N(11)	2.010(6)	Ni(2)−O(6)	2.127(5)
Ni(1)−N(21)	2.019(6)	Ni(2)−O(7)	2.097(5)
Ni(1)−O(1)	1.918(5)	Ni(2)−O(52)	2.027(5)
Ni(1)−O(1)−Ni(2)	129.1(3)	N(2)−Ni(2)−O(52)	174.2(2)
		N(31)−Ni(2)−O(1)	99.2(2)
N(1)−Ni(1)−N(11)	79.2(2)	N(31)−Ni(2)−O(6)	168.1(2)
N(1)−Ni(1)−N(21)	81.3(2)	N(31)−Ni(2)−O(7)	87.2(2)
N(1)−Ni(1)−O(1)	83.4(2)	N(31)−Ni(2)−O(52)	96.4(2)
N(1)−Ni(1)−O(51)	179.1(2)	O(1)−Ni(2)−O(6)	89.1(2)
N(11)−Ni(1)−N(21)	104.6(3)	O(1)−Ni(2)−O(7)	170.1(2)
N(11)−Ni(1)−O(1)	133.2(2)	O(1)−Ni(2)−O(52)	95.5(2)
N(11)−Ni(1)−O(51)	100.0(2)	O(6)−Ni(2)−O(52)	91.2(2)
N(21)−Ni(1)−O(1)	115.2(2)	O(6)−Ni(2)−O(7)	83.5(2)
N(21)−Ni(1)−O(51)	99.1(2)	O(7)−Ni(2)−O(52)	91.1(2)
O(1)−Ni(1)−O(51)	97.1(2)		
N(2)−Ni(2)−N(31)	78.6(2)	O(51)−C(50)−O(52)	127.3(7)
N(2)−Ni(2)−O(1)	82.4(2)	C(50)−O(51)−Ni(1)	133.1(5)
N(2)−Ni(2)−O(6)	94.1(2)	C(50)−O(52)−Ni(2)	132.9(5)
N(2)−Ni(2)−O(7)	91.6(2)		

$[Ni_2(bpepO)(MeCOO)(H_2O)_2](ClO_4)_2 \cdot H_2O \cdot Et_2O \cdot 2EtOH$, 4. Compound **4** crystallizes in the centrosymmetric space group *C*2/*c*. The asymmetric unit contains a single formula unit of **4**. The cation contains the novel asymmetric ligand bpepOH. The structure of the cation of **4** is shown in Figure 5, and selected bond lengths and angles are given in Table 5. The coordination geometries of the Ni(II) ions in the dinuclear center are largely different from each other. The Ni(II) ions are bridged by the alkoxo donor atom O(1) of the ligand and a single acetate anion. In contrast to the planar conformation of this unit in **2** and **3**, the central ring system is folded. Further bridging takes place by a neutral water molecule O(6). The water molecule bridges the two metal ions asymmetrically leading to a rather long bond distance to the sterically encumbered Ni(1) (Ni(1)−O(6) = 2.394(3) Å; Ni(2)−O(6) = 2.176(3) Å). Structural evidence for a neutral bridging water molecule comes from comparison of the Ni−O bond lengths in the same molecule. The average for the Ni−O bond distance of the bridging alkoxo donor atom

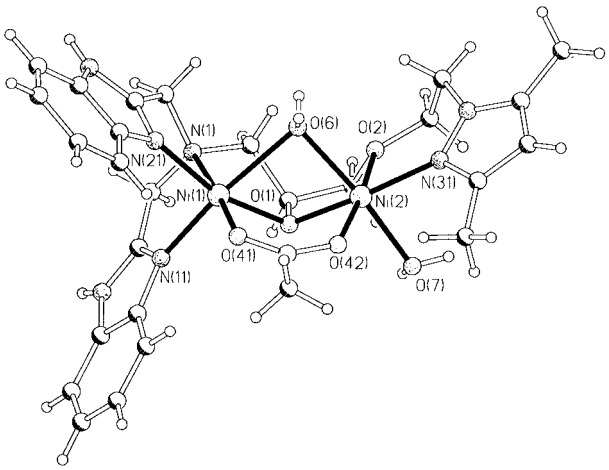

Figure 5. Structure of the cation of $[Ni_2(bpepO)(MeCOO)(H_2O)_2](ClO_4)_2 \cdot H_2O \cdot Et_2O \cdot 2EtOH$, **4**, with selected atomic designations.

Table 5. Selected Bond Lengths (Å) and Angles (deg) for **4**

Ni(1)···Ni(2)	3.171(3)	Ni(1)−O(41)	1.992(3)
		Ni(2)−N(31)	2.098(4)
Ni(1)−N(1)	2.167(4)	Ni(2)−O(1)	2.036(3)
Ni(1)−N(11)	2.028(4)	Ni(2)−O(2)	2.072(3)
Ni(1)−N(21)	2.022(4)	Ni(2)−O(6)	2.176(3)
Ni(1)−O(1)	2.030(3)	Ni(2)−O(7)	2.064(3)
Ni(1)−O(6)	2.394(3)	Ni(2)−O(42)	1.993(3)
Ni(1)−O(1)−Ni(2)	102.53(13)	N(31)−Ni(2)−O(2)	90.07(13)
Ni(1)−O(6)−Ni(2)	87.76(10)	N(31)−Ni(2)−O(6)	99.63(13)
		N(31)−Ni(2)−O(7)	87.46(13)
N(1)−Ni(1)−N(11)	81.7(2)	N(31)−Ni(2)−O(42)	97.00(14)
N(1)−Ni(1)−N(21)	81.42(14)	O(1)−Ni(2)−O(2)	79.22(11)
N(1)−Ni(1)−O(1)	83.50(13)	O(1)−Ni(2)−O(6)	81.49(11)
N(1)−Ni(1)−O(6)	97.17(12)	O(1)−Ni(2)−O(7)	91.25(12)
N(1)−Ni(1)−O(41)	176.56(13)	O(1)−Ni(2)−O(42)	93.72(12)
N(11)−Ni(1)−N(21)	94.9(2)	O(2)−Ni(2)−O(6)	88.58(11)
N(11)−Ni(1)−O(1)	95.45(13)	O(2)−Ni(2)−O(7)	89.86(12)
N(11)−Ni(1)−O(6)	171.89(12)	O(2)−Ni(2)−O(42)	172.92(12)
N(11)−Ni(1)−O(41)	95.7(2)	O(6)−Ni(2)−O(7)	172.74(12)
N(21)−Ni(1)−O(1)	160.26(13)	O(6)−Ni(2)−O(42)	89.80(12)
N(21)−Ni(1)−O(6)	92.86(13)	O(7)−Ni(2)−O(42)	90.88(13)
N(21)−Ni(1)−O(41)	96.64(14)		
O(1)−Ni(1)−O(6)	76.44(11)	O(41)−C(41)−O(42)	126.2(4)
O(1)−Ni(1)−O(41)	99.00(12)	C(41)−O(41)−Ni(1)	128.7(3)
O(41)−Ni(1)−O(6)	85.74(12)	C(41)−O(42)−Ni(2)	131.7(3)
N(31)−Ni(2)−O(1)	169.23(13)		

O(1) is 2.033 Å, which is significantly shorter then the average Ni−O(6) bond distances (average Ni−O = 2.285 Å). Furthermore, the bond length of the terminally coordinated water molecule O(7) (Ni(2)−O(7) = 2.064(3) Å) is even shorter than for both of the Ni−O bonds of the bridging water molecule. The coordination sphere of Ni(1) consists of three nitrogen donor atoms of the bulky, benzimidazolyl-substituted side groups. The coordination geometry is that of an distorted octahedron or that of a square pyramid depending on whether the elongated bond to the bridging water molecule is counted or not. The less distorted octahedral coordination environment of Ni(2) mainly consists of oxygen donor atoms. The coordination shell is completed by the ether oxygen O(2) and the pyrazolyl nitrogen donor of the ligand. The water molecules O(6) and O(7) are in *trans* positions within the coordination polyhedron of Ni(2). The donor atoms of the ligand are in *meridional* positions to each other. In contrast, the structurally similar dinuclear unit of **3** shows the loosely bonded ethanol molecules to be *cis* to each other, and the ligand coordinates in a *facial* mode.

Looking at the structure of urease from *K. aerogenes* it seems to be very likely that a μ-carboxylate−μ-hydroxo dinuclear species forms under physiological conditions. A simple rela-

(20) (a) Satcher, J. H.; Droege, M. W.; Weakley, T. J. R.; Taylor, R. T. *Inorg. Chem.* **1995**, *34*, 3317. (b) Droege, M. W.; Satcher, J. H., Jr.; Reibold, R. A.; Weakley, T. J. R.; Chauffe, L.; Watkins, B. E. *Prepr. Pap. Am. Chem. Soc., Div. Fuel Chem.* **1992**, *37*, 1534.

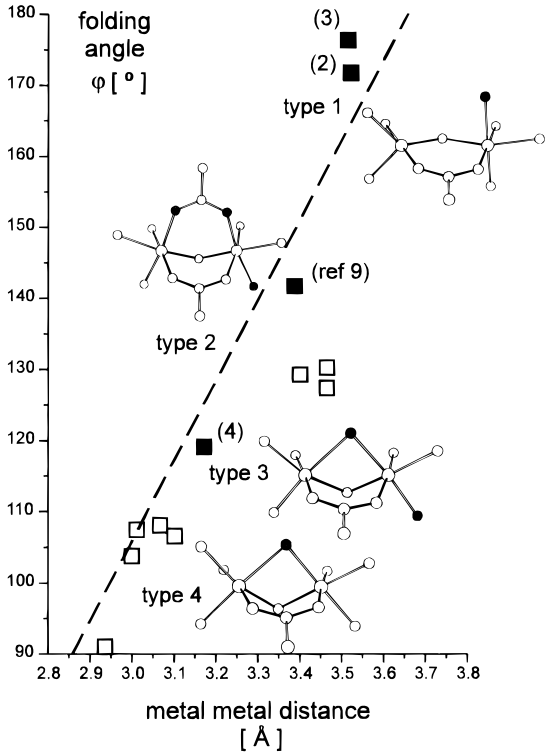

Figure 6. Diagram correlating the folding of the central six-membered (μ_2-(alk-)oxo)(μ_2-carboxylato)dinickel unit with the nonbonding distance between the metal ions. (The folding angle φ of the central six-membered ring system is defined as the angle between the least-squares plane through the metal ions and the atoms of the bridging carboxylate function on the one hand, and the plane that is defined by the the metal ions and the bridging oxygen on the other hand. Filled squares and displayed dinuclear units refer to structure types presented in this or earlier works.[21]

tionship that allows one to describe the conformational changes of such a dinuclear unit is the correlation between the folding angle φ and the nonbonding metal−metal distance, which we found to be *linear* to a good approximation (cf. Figure 6).

Looking for other Ni(II) complexes that possess the μ-carboxylate−μ-hydroxo-bridged moiety, we noticed that the range of all possible conformations is not covered continuously. There seem to be preferred areas that may be assigned tentatively to one of the following structure types.[21] Type 1: planar μ_2-(alk-)oxo-μ_2-carboxylato dinickel unit, where at least one of the metal ions is five-coordinate; typical values are Ni···Ni = 3.5−3.7 Å and φ = 170−180°. Type 2: "half-folded" μ_2-(alk-)oxo−μ_2-carboxylato−dinickel unit comprising an additional μ_2-bridging carboxylate, with both metal ions within a distorted octahedral coordination environment; typical values are Ni···Ni = 3.4−3.5 Å and φ = 120−140°. Type 3: "half-folded" μ_2-(alk-)oxo−μ_2-carboxylato−dinickel unit bridged by a water molecule, with both metal ions within a distorted octahedral coordination sphere; typical values are Ni···Ni ≥ 3.2 Å and $\varphi \geq 120°$.[22] Type 4: completely folded μ_2-(alk-)oxo−μ_2-carboxylato−dinickel unit bridged by an (alk-)oxo anion, with both metal ions within a distorted octahedral coordination environment; typical values are Ni···Ni = 2.9−3.1 Å and φ = 90−110°. It should be noted that the asymmetric dinuclear units of compounds **2** and **3** easily fit into this scheme. Thus, the formation of the asymmetric dinickel unit in **2** and **3** must have energetic reasons that favor its spontaneous formation rather than the comparable symmetric unit. It may also be noted, that the reported Ni···Ni distance of 3.5 Å for the active site of urease from *K. aerogenes* is consistent with a structure type that is intermediate between types 1 and 2. It may be assumed that the enzyme in fact stabilizes the tetrahedral intermediate that forms by the attack of an hydroxide anion on the urea molecule and that this intermediate bridges the μ_2-(alk-)oxo−μ_2-carboxylato−dinickel moiety.

Magnetic Susceptibility Measurements. The temperature dependency of the molar susceptibilities and the effective magnetic moments of compounds **1**−**4** are shown in Figure 7. For **1** and **4**, the effective magnetic moment per Ni ion *decreases* gradually with decreasing temperature. Such behavior can be referred to the presence of an *antiferromagnetic* exchange interaction. In **1**, however, this interaction is not so pronounced since no characteristic maximum in the $\chi(T)$ curve was observed. In **2** and **3**, the $\mu_{eff}(T)$ function first *increases* with decreasing temperature and passes through a maximum at 18 K (**2**) and 19 K (**3**), clearly indicating the existence of a *ferromagnetic* exchange interaction between the Ni centers. The experimental data were fitted to eq 1 on the basis of the isotropic spin-

$$\chi = (1 - x_p)\,\chi_{dim} + 2x_p\chi_{mono} + 2N_\alpha \qquad (1)$$

Hamiltonian $\hat{H} = -2J\hat{S}_1\hat{S}_2$ with $S_1 = S_2 = 1$ without zero-field splitting for the dimer,[23,24] where the susceptibility is expressed per nickel dimer. Here x_p is the molar fraction of paramagnetic impurities, N_α refers to the temperature-independent paramagnetism (200×10^{-6} cm^3/mol per Ni(II)), and D describes the zero-field-splitting of the monomeric impurities. For the ferromagnetic coupled dimers **2** and **3**, a Weiss Θ constant was included to describe phenomenologically the decrease of $\mu_{eff}(T)$ at low temperatures. The parameters obtained from nonlinear fits of the experimental data to eq 1 are given in Table 6.

(21) The following compounds were taken into the diagram. type 1: **2**, Ni···Ni = 3.52 Å, φ = 171.8°; **3**, Ni···Ni = 3.51 Å, φ = 176.4°. type 2: $[Ni_2(L)(PhCOO)_2(MeCOOH)]^+$, LH = 1-[bis(2-pyridylmethyl)amino]-3-[2-(2-pyridyl)ethoxy]-2-hydroxypropane, Ni···Ni = 3.39 Å, φ = 141.7°;[9] $[Ni_2(bbapO)(MeCOO)_2]^+$, Ni···Ni = 3.46 Å, φ = 130.3°. (a) Hommerich, B. Diploma thesis, Münster, 1994. $[Ni_2(L)_2(OH)(MeCOO)_2]^+$, L = *N*,*N*′,*N*″-trimethyl-1,4,7-triazacyclononane, Ni···Ni = 3.40 Å, φ = 129.3°. (b) Chauduri, P.; Küppers, H.-J.; Wieghardt, K.; Gehring, S.; Haase, W.; Nuber, B.; Weiss, J. *J. Chem. Soc., Dalton Trans.* **1988**, 1367. $[Ni_2(L)(MeCOO)_2]^+$, LH = 2,6-bis-[(bis((1-methylimidazol-2-yl)methyl)amino)methyl)]-4-methylphenol, Ni···Ni = 3.46 Å, φ = 127.4°. (c) Buchanan, R. M.; Mashuta, M. S.; Oberhausen, K. J.; Richardson, J. F.; Li, Q.; Hendrickson, D. N. *J. Am. Chem. Soc.* **1989**, *111*, 4497. type 3: **4**, Ni···Ni = 3.17 Å, φ = 119.1°. type 4: $[Ni_3(L)_2(MeCOO)_2]^{2+}$, LH = 1-[*N*,*N*-bis-(benzimidazol-2yl-methyl)]amino-2,3-dihydroxypropane, Ni···Ni = 3.08 Å, φ = 107.5°. (d) Volkmer, D. Ph. D. Thesis, Münster, 1994. $[Ni_4(L)(\mu_4\text{-}OH)(\mu_2\text{-}OMe)(MeCOO)_2(\mu_2\text{-}MeOH)]$, LH_4 = *N*,*N*′-bis(2,6-diformyl-4′-methylphenol)bis(2,6-bis(aminomethyl)-4-methylphenol, Ni···Ni = 2.94 Å, φ = 91.0°. (e) Bell, M.; Edwards, A. J.; Hoskins, B. F.; Kachab, E. H.; Robson, R. *J. Am. Chem. Soc.* **1989**, *111*, 3603. $[Ni_4(\mu_3\text{-}OMe)_4(L)_4(MeCOO)_2]^{2+}$, L = 2,5-dimethyl-2,5-diisocyanohexane, Ni···Ni = 2.99 Å, φ = 103.8°. (f) Gladfelter, W. L.; Lynch, M. W.; Schaefer, W. P.; Hendrickson, D. N.; Gray, H. B. *Inorg. Chem.* **1981**, *20*, 2390. $[Ni_2(L)_2(MeCOO)(MeCN)_2]^+$, LH = 2-(2-hydroxyphenyl)-1,10-phenanthroline, Ni···Ni = 3.01 Å, φ = 107.5°. (g) Holligan, B. M.; Jefferey, J. C.; Ward, M. D. *J. Chem. Soc., Dalton Trans.* **1992**, 3337. $[Ni_2(L)_4(MeCOO)]^-$, LH = *N*-phenylsalicylaldimine, Ni···Ni = 3.10 Å, φ = 106.6°. (h) Butcher, R. J.; O'Connor, C. J.; Sinn, E. *Inorg. Chem.* **1982**, *21*, 661.

(22) Since compound **4** was the only example for type 3 that we were actually aware of, we did not think it right to assign typical values for that structure type.

(23) O'Connor, C. D. *Prog. Inorg. Chem.* **1982**, *29*, 239.

(24) Theoretical expressions used to calculate magnetic susceptibility data:

$$\chi_{dim} = \left(\frac{N_L g^2 \mu_B{}^2}{kT}\right)\frac{2\exp(2J/kT) + 10\exp(6J/kT)}{1 + 3\exp(2J/kT) + 5\exp(6J/kT)}$$

$$\chi_{mono} = \left(\frac{2\,N_L g^2 \mu_B{}^2}{3\,kT}\right)\frac{(2kT/D) + 2\exp(-D/kT)/(D/kT) + \exp(-D/kT)}{1 + 2\exp(-D/kT)}$$

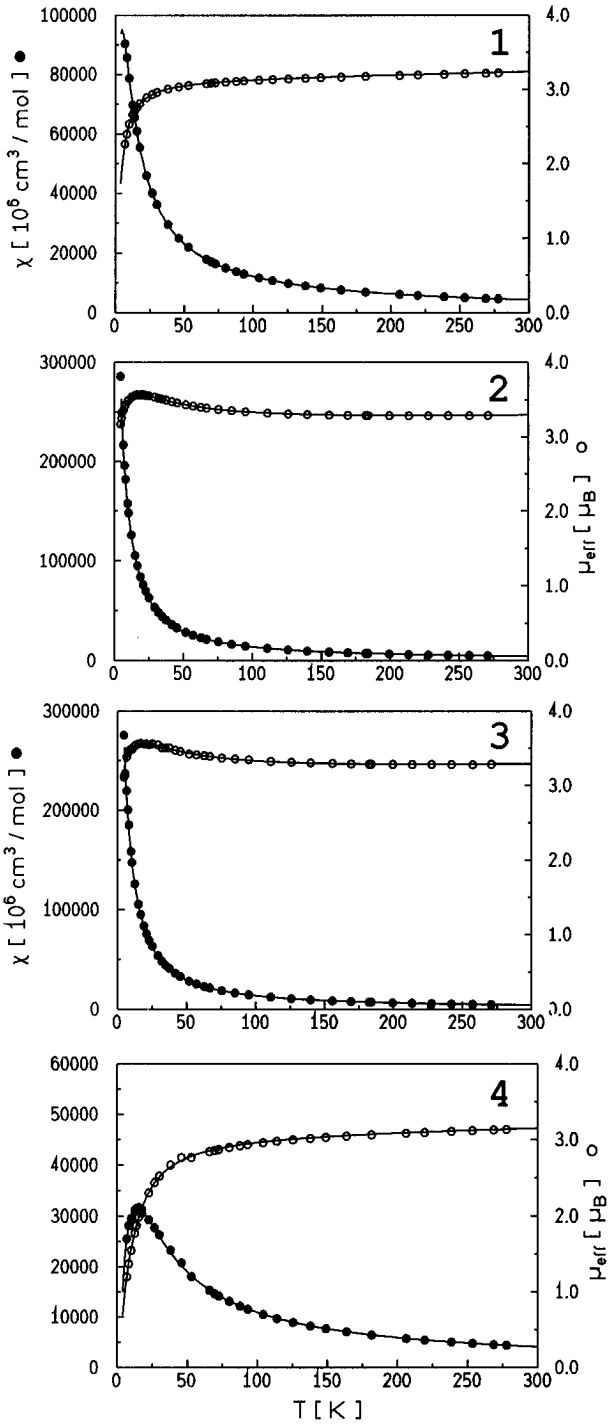

Figure 7. Temperature dependence of the corrected molar magnetic susceptibility χ_M and the experimental magnetic moment per dimer of compounds **1**−**4**.

Table 6. Fit Parameters of the Susceptibility Measurements of Compounds **1**−**4**

complex	J^a	g^b	$x_p{}^c$	Θ^d	$D_p{}^e$
1	−1.8(1)	2.21(1)	<0.01		0.0(1)
2	7.7(1)	2.20(1)	0.3(1)	−1.9	−7.6(1)
3	7.8(1)	2.20(1)	<0.01	−1.9	−6.1(1)
4	−5.3(1)	2.17(1)	1.2(1)		−0.4(1)

[a] J = coupling constant (cm^{-1}). [b] $g = g$ value of the nucleus. [c] x_p = molar fraction of paramagnetic impurity (%). [d] Θ = Weiss constant (K). [e] D_p = zero-field splitting of the monomeric impurities (cm^{-1}).

While antiferromagnetic coupling between μ-oxo-bridged dinuclear Ni(II) complexes is often observed,[21b,c;25] the presence of a ferromagnetic exchange interaction in **2** and **3** is quite unusual. Although the metal distances in the dinuclear structure units of **2** and **3** are rather long (Ni(1)···Ni(2) = 3.521(4) Å (**2**); Ni(1)···Ni(2) = 3.514(3) Å (**3**)) and, as a consequence, the μ-oxo bridge is opened wide (Ni(1)−O(1)−Ni(2) = 128.2(2)° (**2**); Ni(1)−O(1)−Ni(2) = 129.1(3)°, (**3**)), we had to rule out the possibility of a different exchange mechanism due to these structural features, since the structurally similar compound **1** showed antiferromagnetic coupling between the Ni(II) ions (Ni(1)···Ni(2) = 3.734(3) Å, Ni(1)−O(1)−Ni(2) = 129.1(2)°). The ferromagnetic behavior of compounds **2** and **3** may be ascribed to the 5-fold coordination of one of the Ni(II) ions. However, since it is hard to prove the conservation of the dinuclear structure as resulting from X-ray structure analysis under the experimental conditions of the magnetic measurements, we abstain from further explanations.[26] It should be noted though, that we found it impossible to derive a correlation between the coupling constant J and any kind of structural parameter of the dinuclear Ni(II) complexes. This contrasts with the observation for structurally similar, μ-oxo-bridged dinuclear Fe(III) complexes where a correlation between the magnitude of J and the metal−μ-oxo bond length has been described.[27]

Table 7. Electronic Absorption Properties of Compounds **1**−**4**

complex	$\lambda_{max}{}^a$	$\epsilon_{max}{}^b$	⟨av/Ni⟩[c]
1	380, sh		
(MeOH)	653 (641)	23.4	
	1024 (1090)	23.3	3N, 3O
2	405 (408)	59.0	
(MeOH)	495, sh (504)	(nd)	
	646 (654)	38.3	
	771 (795)	16.4	
	1030 (1038)	36.5	2.5N, 3O
3	402 (424)	57.9	
(EtOH)	648 (673)	33.0	
	1074 (1050)	32.2	2.5N, 3O
4	410 (395)	58.1	
(EtOH)	660 (633)	27.6	
	762 (761)	18.2	
	1043 (1008)	25.7	2N, 4O

[a] λ_{max} = absorption maximum (nm); reflectance data in parantheses. [b] ϵ_{max} = molar absorption coefficient (M^{-1} cm^{-1}). [c] ⟨av/Ni⟩ = average donor environment per nickel(II) ion. sh = shoulder; nd= not determinable.

Electronic Absorption Properties. The data for the absorption spectra of compounds **1**−**4** are listed in Table 7. Complexes **2** and **3** showed no significant change in the absorption spectra by comparison with the band maxima and band shapes of their solid state reflectance spectra. Hence, it seems to be very likely that the five-coordination of one of the Ni(II) ions remains in solution.

Complex **4** shows changes in the absorption spectrum by means of a shift of the band maximum of the middle transition and an increase of the absorption intensities that make its absorption properties in solution quite similar to those of complexes **2** and **3**. Although the appearance of the spectra bears similarities with those for octahedrally coordinated Ni(II) ions, the assignment of the three most intense bands to the spin-allowed transitions from the $^3A_{2g}$ ground state of an octahedrally coordinated d^8 ion to the next higher excited triplet states ($^3T_{1g}$-

(25) Turpeinen, U.; Hämäläinen, R.; Reedijk, J. *Polyhedron* **1987**, *6*, 1603.
(26) For magnetic susceptibility measurements the compounds were powdered and dried under high vacuum in order to remove the solvent molecules which are included in the crystal lattice. We cannot rule out the possibility of changes in the coordination of the Ni(II) ions due to the treatment of the samples, e.g. the terminally coordinated oxygen donors O(6) in the structures of **2** and **3** may become bridging ligands or dissociate off.
(27) Gorun, S. M.; Lippard, S. J. *Inorg. Chem.* **1991**, *30*, 1625.

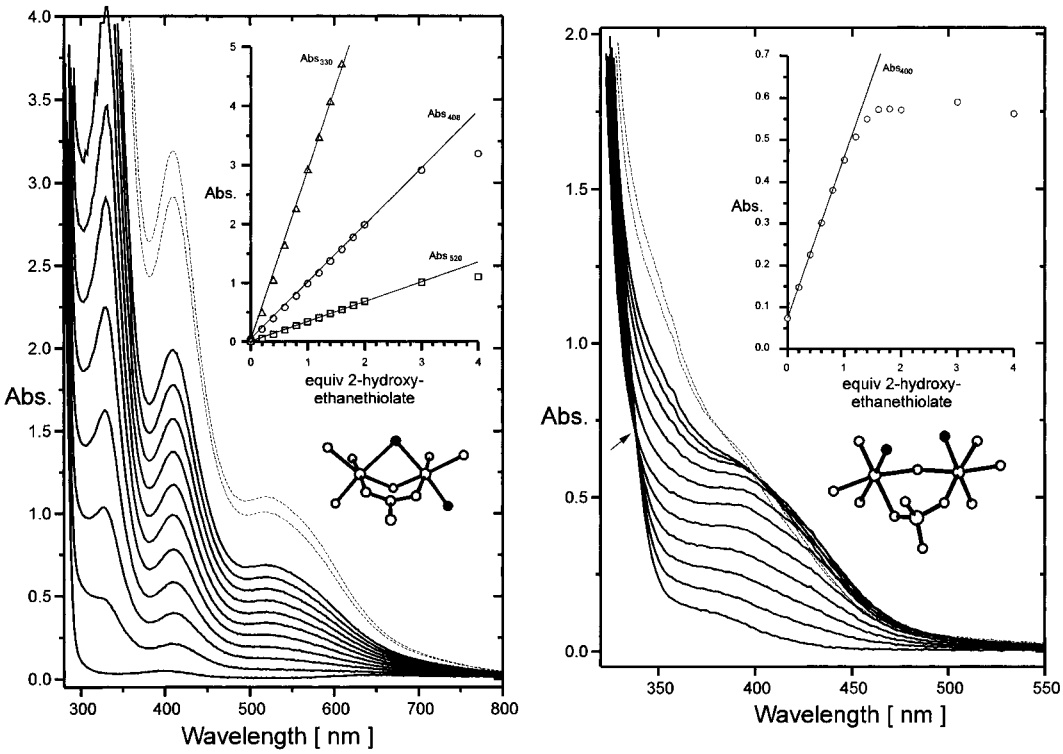

Figure 8. Electronic spectra of compounds **4** (left) and **1** (right) in the presence of different amounts of sodium 2-hydroxy-ethanethiolate (2-MEat). Solid lines correspond to molar ratios of the complexes: 2-hydroxy-ethanethiolate (0, 0.2, 0.4...2.0 equiv 2-MEat), dashed lines display the spectra in the presence of 3.0 and 4.0 equiv 2-MEat. The insets show the changes in absorbance for the different concentrations of 2-MEat at the absorption maxima.

(P), $^3T_{1g}$(F) and $^3T_{2g}$(F)) would be a misinterpretation. The *Dq* values of complexes **2**−**4** that are either calculated from the energy of the transitions $^3A_{2g} \rightarrow {}^3T_{1g}$(P) and $^3A_{2g} \rightarrow {}^3T_{1g}$(F) or directly read from the lowest energy transition differ significantly, which should not be the case for octahedrally coordinated Ni(II) ions.[28] Furthermore, the molar extinction coefficients of the absorption band maxima of **2**−**4** are unusually high. The spectra in fact indicate a trigonal bipyramidal coordination environment of at least one of the Ni(II) ions.[29]

The spectral properties of jack bean urease have constantly been assigned to the transitions of Ni(II) ions in an octahedral coordination environment.[30] However, if the $^3A_{2g} \rightarrow {}^3T_{1g}$(P) and the $^3A_{2g} \rightarrow {}^3T_{1g}$(F) transitions are taken into account, the calculated *Dq* values would uniformly indicate an average donor environment which is particularly rich in oxygen, which would be in contradiction to the results of enzymological studies.[31] As a summary we conclude that the spectral properties of the jack bean urease are rather consistent with Ni(II) ions in a trigonal bipyramidal coordination sphere. Further evidence comes from the crystal structure of urease from *K. aerogenes* which shows a trigonal bipyramidal coordination of Ni(2) with two histidine ligands.[7]

Table 8. Spectral Parameters of Urease and of Complexes **1**−**4** in the Presence of 2-Mercaptoethanol[a]

specimen	$\lambda_{max,1}$ ($\epsilon_{max,1}$)	$\lambda_{max,2}$ ($\epsilon_{max,2}$)	$\lambda_{max,3}$ ($\epsilon_{max,3}$)
Jack bean[32a]	324 (1550)	380 (890)	420 (460)
K. aerogenes[32b]	322 (2230)	374 (1060)	432 (530)
1[32c]	310	400 (450)	
2	329 (185)	406 (68.5)	513 (14.4)
3	331 (1051)	410 (349)	521 (120)
4	330 (2900)	408 (990)	520 (340)

[a] $\lambda_{max,n}$ = absorption maximum [nm] (ϵ_{max} = molar absorption coefficient [M^{-1} cm^{-1}]).

The electronic spectra of the ureases from jack beans and *K. aerogenes* in the presence of mercaptoethanol show three characteristically intense absorption bands in the ultraviolet region which have been assigned to thiolate → Ni(II) charge transfer transitions. Table 8 shows the spectral data of the enzymological investigations together with the results of the titration of compounds **1**−**4** with 2-hydroxyethanethiolate (2-MEat).

The titration experiment proved to be a very sensitive method for the characterization of the complexes. As an illustration

(28) Underhill, A. E., Billing, D. E. *Nature* **1966**, *210*, 834.

(29) (a) Ciampolini, M. *Inorg. Chem.* **1966**, *5*, 35. (b) Sacconi, L.; Ciampolini, M.; Speroni, G. P. *J. Am. Chem. Soc.* **1965**, *87*, 3102. (c) Ciampolini, M.; Nardi, N. *Inorg. Chem.* **1966**, *5*, 41.

(30) Spectroscopic data for jack bean urease have been reported as follows: (a) $^3A_{2g} \rightarrow {}^3T_{1g}$(P), 407 nm (208 M^{-1} cm^{-1}); 630 nm (sh); $^3A_{2g} \rightarrow {}^3T_{1g}$(F), 745 nm (46 M^{-1} cm^{-1}); 820 nm (sh); 910 nm (14 M^{-1} cm^{-1}); $^3A_{2g} \rightarrow {}^3T_{2g}$, 1060 nm (10 M^{-1} cm^{-1}). Data are related to one 96.6 kDa subunit that comprises two Ni(II) ions.[8e] (b) $^3A_{2g} \rightarrow {}^3T_{1g}$(P), 425 nm (<95 M^{-1} cm^{-1}); $^3A_{2g} \rightarrow {}^3T_{1g}$(F), 750 nm (30 M^{-1} cm^{-1}); $^3A_{2g} \rightarrow {}^3T_{2g}$, 1020 nm (20 M^{-1} cm^{-1}). Data are related to the absolute concentration of Ni(II) ions in the solution.[8c] (c) $^3A_{2g} \rightarrow {}^3T_{1g}$(P), 420 nm; $^3A_{2g} \rightarrow {}^3T_{1g}$(F), 745 nm; $^3A_{2g} \rightarrow {}^3T_{2g}$, 1300 nm. Magnetic circular dichroism study: Finnegan, M. G., Kowal, A. T.; Werth, M. T.; Clark, P. A.; Wilcox, D. E.; Johnson, M. K. *J. Am. Chem. Soc.* **1991**, *113*, 4030.

(31) The primary structure of the ureases from *P. mirabilis*, *H. pylori*, *K. aerogenes*, and jack beans have a common conservative sequence of 20 amino acid residues. Among those three histidine residues are found that are expected to be directly coordinated to the metal ions; cf. ref 5.

(32) Conditions employed: (a) pH = 7.12, T = 25 °C, absorption coefficient related to the 96.6 kDa subunit that comprises two Ni(II) ions, stoichiometric ratio of 2-mercaptoethanol/96.6 kDa subunit 92:1.[8e] (b) pH = 7.75, *T* = 25 °C, absorption coefficient related to M_r = 224 kDa with four Ni(II) ions, varying stoichiometric ratio, absorption coefficient extrapolated to an indefinitely high excess of 2-mercaptoethanol.[14a] (c) Nonbuffered solutions of the complexes in MeOH, titrations with sodium 2-hydroxyethanethiolate, absorption coefficient related to the stoichiometric ratio of the complex/2-hydroxyethanethiolate of 1:1.

for the different behavior, the titration spectra of complexes **4** and **1** are displayed in Figure 8. Complexes **2**−**4** yield similar titration spectra. In contrast to the enzymes only two CT absorption bands develop in the region between 320 and 430 nm. An additional absorption band develops at 520 nm which is not found for the enzymes. The identity of the band maxima for titrations of complexes **2**−**4** led us to the conclusion that the same species is formed under these conditions. Crystallization experiments to isolate a dinuclear thiolate-bridged complex yielded in contrast to our expectations black crystals of the cyclic hexamer $[Ni_6(SCH_2CH_2OH)_{12}]$.[33]

The titration spectra of complexes **2**−**4** may be explained by the formation of mononuclear Ni(II) complexes of the polydentate ligands. As an example, the stoichiometry of the complex formation during titration of **4** may be

$$[Ni_2(bpepO)(MeCOO)(H_2O)_2]^{2+} + (n/3)HOCH_2CH_2S^- \rightarrow [Ni(bpepOH)(OH)]^+ + (1/n)[Ni_n(SCH_2CH_2OH)_{2n}] + MeCOO^- + H_2O,$$

where $[Ni_n(SCH_2CH_2OH)_{2n}]$ represents a coordination polymer of Ni(II) in which the square planar coordination planes of the Ni(II) ions are bridged by the thiolate sulfurs.[34] From the different extinction coefficients of compounds **2**−**4** in the presence of 1 equiv of 2-MEat it appears that the dinuclear precursor complexes have different stabilities. Thus, a metal ion is readily extruded from **4**, while significant changes in the titration spectra of **2** only appeared after more than 2 equiv of 2-MEat having been added to the solution. In all cases, the titrand 2-MEat was not suited to estimate the "free" coordination sites, since dissociation of the dinuclear complexes occured.

In contrast, the titration spectrum of **1** yields only two new bands in the region 300−800 nm. The more intense band at 310 nm overlays the already existing band at 309 nm which is probably due to a phenolate → Ni(II) CT (ϵ_{max} = 3340 M^{-1} cm^{-1}). The increase of the absorption maximum at 400 nm shows a linear increase until 1 equiv of 2-MEat is added. It is very likely that a single species forms under these conditions, since the titration spectrum shows an isosbestic point (λ = 339 nm, ϵ = 680 M^{-1} cm^{-1}) up to the molar ratio of 1:1. Further addition of thiolate results in a saturation behavior of the system. No significant increase of the absorption at 400 nm could be observed if more than 2 equiv of 2-MEat had been added. A possible structural model could be envisaged where a thiolate-bridged dinuclear complex contains two five-coordinated Ni(II) ions. However, all attempts to isolate crystals suitable for X-ray crystallographic investigations have failed so far.

Kinetic Investigations. Progress in the development of metal complex catalyzed hydrolysis of appropriate substrates have been reviewed recently.[35] Our aim was to find the appropriate conditions that would allow us to quickly screen the synthesized complexes on their different hydrolytic activity toward certain test substrates. We have used the common spectrophotometric method which makes use of the readily detectable chromophoric leaving groups *p*-nitrophenol (pnp) and *p*-nitroaniline (pna). The test substrates 4-nitrophenyl phosphate (pnpp), bis(4-nitrophenyl)phosphate (bpnpp) and 4-nitroacetanilide (pnaa) have been used extensively in hydrolysis studies.[36] To unify the hydrolysis experiments we also employed (4-nitrophenyl)urea (pnpu) in our studies, which is *not* a test substrate for urease activity in enzymological studies.[37]

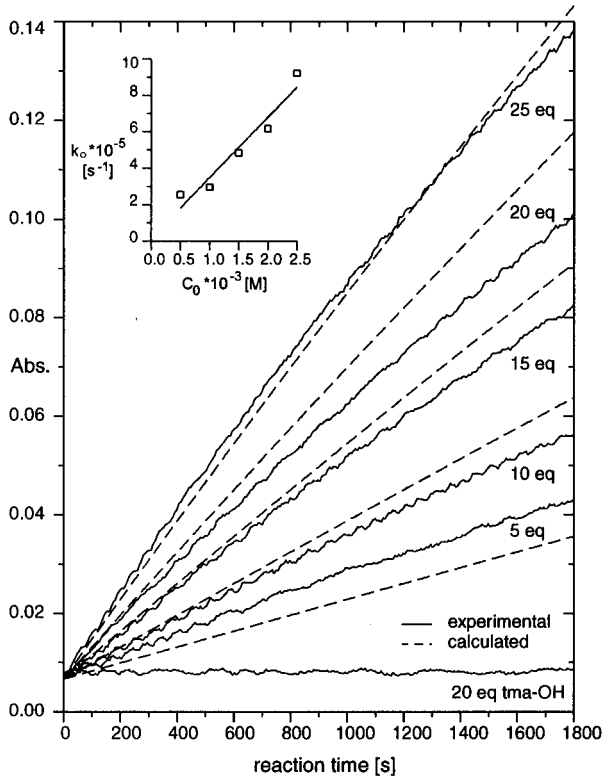

Figure 9. Time course for the change in absorbance for the hydrolysis of 4-nitrophenyl-phosphate (pnpp) by compound **4**. Conditions: c_0(pnpp) = 1.0 × 10^{-4} M, c_0(**4**) = c_0(tetramethylammonium hydroxide) = 2.5 × 10^{-3}, 2.0 × 10^{-3}, 1.5 × 10^{-3}, 1.0 × 10^{-3}, 0.5 × 10^{-3} M, λ = 400 nm, T = 60 °C, methanol solvent. The baseline shows the change in absorbance in absence of **4** (c_0(tma-OH) = 2.0 × 10^{-3} M). The inset shows the dependence of the observed pseudo first-order rate constant k_o from the different starting concentrations c_0 of the catalyst. The dashed lines represent simulations corresponding to eq 7 in ref 17 using the parameters ϵ_{pnpat} = 9870 M^{-1} cm^{-1} and k_2 = 0.033 M^{-1} s^{-1} with m = 1.

The comparative hydrolysis studies of the synthesized metal complexes gave the following results: Among the investigated catalysts, complex **4** exclusively showed a notable acceleration of the test substrate hydrolysis, and a remarkable substrate selectivity for the activated phosphate *mono*ester pnpp (cf. Figure 9). The standard nature of the reaction of **4** with pnpp

(33) (a) Gould, R. O.; Harding, M. M. *J. Chem. Soc. A* **1970**, 875. (b) Spectral data for the structurally similar complex $[Ni_6(SCH_2CH_2CH_3)_{12}]$ are as follows: $\lambda_{max,1}$ = 336 nm ($\epsilon_{max,1}$ = 58 000 M^{-1} cm^{-1}), $\lambda_{max,2}$ = 408 nm ($\epsilon_{max,2}$ = 20 500 M^{-1} cm^{-1}), $\lambda_{max,3}$ = 555 nm ($\epsilon_{max,3}$ = 7000 M^{-1} cm^{-1}), Krüger, T. Ph.D. Thesis, Münster, 1990.

(34) The detection of mononuclear complexes of the ligands tbpOH, m-tbpOH, and bpepOH could not be proven by the electronic absorption spectra, which are dominated by the intense CT transitions of the cyclic polymers. Our experiences with complex formation with this kind of ligand show that mononuclear complexes are formed preferentially if no bridging anions are present that stabilize the dinuclear unit (*vide infra*).

(35) (a) Chin, J. *Acc. Chem. Res.* **1991**, *24*, 145. (b) Breslow, R. *Acc. Chem. Res.* **1995**, *28*, 146.

(36) (a) De Rosch, M. A., Trogler, W. C. *Inorg. Chem.* **1990**, *29*, 2409. (b) Koike, T., Kimura, E. *J. Am. Chem. Soc.* **1991**, *113*, 8935. (c) Vance, D. H., Czarnik, A. W. *J. Am. Chem. Soc.* **1993**, *115*, 12165. (d) Akkaya, E. U.; Czarnik, A. W. *J. Phys. Org. Chem.* **1992**, *5*, 1992.

(37) The use of substrates that contain activated leaving groups has been criticized repeatedly. However, the broad use of the mentioned test substrates allows us to compare the hydrolysis efficiency of different model systems and thus has set its own standard. (a) Menger, F. M.; Ladika, M. *J. Am. Chem. Soc.* **1987**, *109*, 3145. (b) Breslow, R.; Singh, S. *Bioorg. Chem.* **1988**, *16*, 408.

(38) Due to the UV-absorption of the ligand bpepO, the observation of the reaction spectrum at wavelengths <300 nm was not possible. Compared to the reaction spectrum of the spontaneous hydrolysis of pnpp in alkaline aqueous solutions the absorption maximum of the released phenolate is shifted to lower energy and lower intensity (λ_{max} = 378 nm, ϵ_{max} = 12 000 M^{-1} cm^{-1}), which is presumably due to the coordination of the phenolate to one of the Ni(II) ions (*vide infra*).

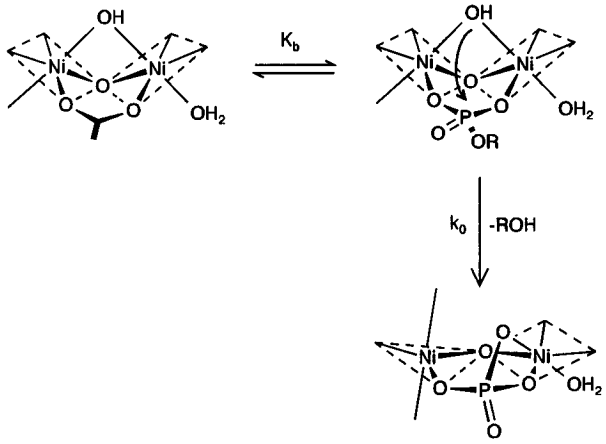

Figure 10. Reaction model for the stoichiometric hydrolysis of the phosphate monoester by the dinuclear complex **4**. K_b represents the equilibrium constant for the exchange of the bridging acetate against a bridging phosphate monoester dianion. The pseudo-first-order rate contant k_o corresponds to the slowest, rate-determining step in the reaction mechanism, which here is arbitrarily assigned to the attack of the bridging hydroxide nucleophile on the phosphorus center.

was tested by monitoring the reaction spectrum in the range of 300−460 nm for 22 h. The reaction spectrum showed a sharp isosbestic point at 341 nm,[38] which strongly indicates a uniform course of the reaction.[39]

Complex **4** promotes the stoichiometric hydrolysis of pnpp in methanolic solution. No significant hydrolysis of the test substrate occured when the metal complex was absent. The results furthermore show that the initial rate of the pnpp test substrate is linearly dependent on the concentration of the catalyst. For the examined range of concentrations we have determined a second-order rate constant $k_2 = 0.033(5)\ M^{-1}\ s^{-1}$ ($T = 60$ °C, uncorrected).[40]

The following simplified reaction model is in accordance with the results obtained so far (cf. Figure 10). In a first step, the bridging water molecule in **4** is rapidly deprotonated by the added stoichiometric amount of hydroxide anions, resulting in a strained, hydroxy-bridged dinuclear complex. The observed reaction then consists of an irreversible step that leads to the fission of the P−OR bond of the phosphate ester and a reversible preequilibrium, which is defined by the equilibrium constant of the coordination of the substrate to the dinuclear metal complex. The kinetic analysis for systems of a single irreversible step with a preequilibrium has been discussed in detail.[41] From the proposed reaction scheme a pseudo-first-order rate law follows if the preequilibrium adapts quickly. Furthermore, the observed rate constant k_o is directly proportional to the bonding constant of the test substrate to the metal complex which may explain why the order of hydrolysis of the test substrates occurs (pnpp > bpnpp ≫ pnaa, pnpu) and does *not* correspond to the order of the thermodynamic stability of the cleaved bonds. The preferential cleavage of the phosphate monoester dianion may thus be regarded as an indirect proof for a dinuclear catalysis. Similar reaction mechanisms have been proposed for the cleavage of phosphate monoesters by dinuclear Co(III) complexes.[42]

The lack of activity of the investigated compounds on urea hydrolysis may also indicate that the acceleration of phosphate ester hydrolysis occurs much easier and that the urease active site is finely tuned for this purpose.

However, further kinetic investigations are underway to establish the reaction mechanism for the hydrolysis of test substrates by the asymmetric dinuclear complex **4** and similar derivatives.

Summary and Conclusions

Novel asymmetric Ni(II) complexes have been synthesized in order to mimic the structure and function of the dinuclear active sites of ureases. Compounds **2** and **3** have one of the nickel ions in a five-coordinated, trigonal bipyramidal coordination environment and thus show a high *structural* similarity to the active site of urease from *K. aerogenes*. The same compounds display unusual physical properties which justifies their designation as urease enzyme models: the UV−vis spectra of the compounds **2** and **3** show a much better correspondence to the spectral properties of the urease enzyme under physiological conditions than regular octahedral Ni(II) complexes do. Furthermore, magnetic susceptibilty measurements show the Ni(II) ions in the dinuclear centers of **2** and **3** to be ferromagnetically coupled in contrast to the antiferromagnetic exchange interaction usually observed for μ-oxo−μ-carboxylato-bridged Ni(II) complexes. The sensitivity of the magnetic behavior against structural changes within the dinuclear center thus mirrors the inconsistent results of magnetic studies on the urease enzyme for which ferromagnetic,[30c] antiferromagnetic,[8c] and nonexchange behavior have been reported.[8b]

Unfortunately, none of the investigated model compounds shows hydrolytic activity toward urea or amide test substrates. In contrast, compound **4** specifically accelerates the hydrolysis of 4-nitrophenyl phosphate in a stoichiometric reaction. A reaction mechanism is proposed in which a bridging hydroxide nucleophile attacks the phosphorus center of the likewise bridging phosphate monoester dianion. Due to the asymmetric structure of the ligand in complex **4**, the metal ions possess differentiated functions. The lack of activity of the structurally similar asymmetric complexes **2** and **3** reveals the importance of an appropriate ligand design. Future investigations will concentrate on adjusting the catalyst properties towards ureolytic activity. One of the main problems to be overcome is the weak bonding of the urea substrate within protic solvents. Also, attachment of polar groups on the ligand periphery may be necessary in order to dissolve the complexes in aqueous medium and thus to facilitate kinetic investigations under enzymological conditions.

Acknowledgment. We are grateful for financial support by the Fonds der Chemischen Industrie and the Deutsche Forschungsgemeinschaft. D.V. thanks the Graduiertenfoerderung NRW for a scholarship. We thank Dr. Thomas Johnson and Dr. Virginia Smith for carefully reviewing the manuscript.

Supporting Information Available: Tables listing crystal data and structure refinement details, atomic coordinates, isotropic and anisotropic thermal parameters, and bond distances and angles for the X-ray structure analysis of compounds **1**−**4** and ORTEP views of the compounds with complete atomic labeling (27 pages). Ordering information is given on any current masthead page.

IC951567X

(39) (a) Mauser, H. Z. *Naturforsch.* **1968**, *23B*, 1025. (b) Lachmann, H.; Mauser, H.; Schneider, F.; Wenck, H. *Z. Naturforsch.* **1971**, *26B*, 629.

(40) Since the hydrolysis rate for the pnpp dianion is constant within the pH range of 9−14, it is not possible to determine a rate constant k_2 for the spontaneous hydrolysis. To compare the systems we recalculated k_o values for the catalyzed reaction for different concentrations of the metal complex. The rate acceleration by the metal complex is by a factor of 20 compared to the spontaneous hydrolysis of pnpp (T = 58 °C, 0.1 M K_2CO_3 buffer), but 1.3×10^5 at pH 14. Kirby, A. J.; Jencks, W. P. *J. Am. Chem. Soc.* **1965**, *87*, 3209.

(41) Beringer, F. M.; Findler, E. M. *J. Am. Chem. Soc.* **1955**, *77*, 3200.

(42) (a) Wahnon, D.; Lebuis, A.-M.; Chin, J. *Angew. Chem.* **1995**, *107*, 2594; *Angew. Chem., Int. Ed. Engl.* **1995**, *34*, 2412. (b) Chin, J.; Banaszczyk, M. *J. Am. Chem. Soc.* **1989**, *111*, 4103.